We are thankful to the two reviewers for their thoughtful comments that help improve the manuscript significantly. Following the reviewers' suggestions, we have revised the manuscript accordingly. Listed below are our point-by-point responses in blue to each reviewer's comments.

Response to Reviewer #1

The manuscript entitled, "Chemical characterization of submicron aerosol and particle growth events at a National Background Site (3295 m a.s.l.) in the Tibetan Plateau" by W. Du et al., presents non-refractory plus black carbon (BC) aerosl chemical composition and particle size distribution data from a remote location on the northeastern region of the Tibetan Plateau. The observations reported here fill a gap of data from this part of the world. The location is very interesting for readers of Atmospheric Chemistry and Physics. The manuscript is generally well-written, yet needs clarification in some areas and additional analysis. Overall, the data were presented well, but much of the interpretation was left to the reader, which makes it difficult to understand the broader picture of the important findings from this study. I recommend publication after addressing these issues.

Thank the reviewer's comments. The manuscript was significantly revised according to the reviewer's suggestions listed below.

Major comments:

The overriding issue is that while the data are from a remote, "background" site, there needs to be some analysis as to where the episodes with high mass concentrations and new particle formation events are coming from. An analysis of the various wind directions and back trajectories would also be helpful in putting these observations in the context of other nearby measurements (in particular, Bird Island at Qinghai Lake and Mt. Waliguan). Throughout the text, there is mention of regional transport being important to observations. From where? I was surprised to find that there are many urban (prefecture) areas within 200 km of the site with populations greater than 500,000 that may be contributing to the background aerosol. This information was not provided in the manuscript. Also, the infrastructure (railroads, agriculture, power plants, etc.) for supporting these people needs to be considered as potential sources.

Thank the reviewer's comments. The back trajectories for the episodes with high aerosol mass loadings are now shown in Fig. S3 in supplementary in the revised manuscript. The new particle formation is formed locally which is initiated by the formation of gas sulfuric acid. In this study, we focus on the particle growth stage rather than new particle formation due to the limitations of SMPS and ACSM measurements. Additional analysis of winds and back trajectories were added in the revised manuscript. In addition, the reasons we didn't compare with the measurements at Bird Island at Qinghai Lake were detailed below. Regional transport is an important contribution to aerosol particles at the rural site. However, this study was not to quantity the contributions of regional transport from different source areas because such analyses need the involvement of modeling work which is beyond the scope of this study. Similarly, the infrastructure (railroads, agriculture, power plants, etc.) might also have impacts on the sampling site, however, without additional measurements, it is difficult to evaluate and quantity their impacts.

Following the reviewer's suggestions, we revised the manuscript as much as we can. Please see our detailed point-to-point responses below.

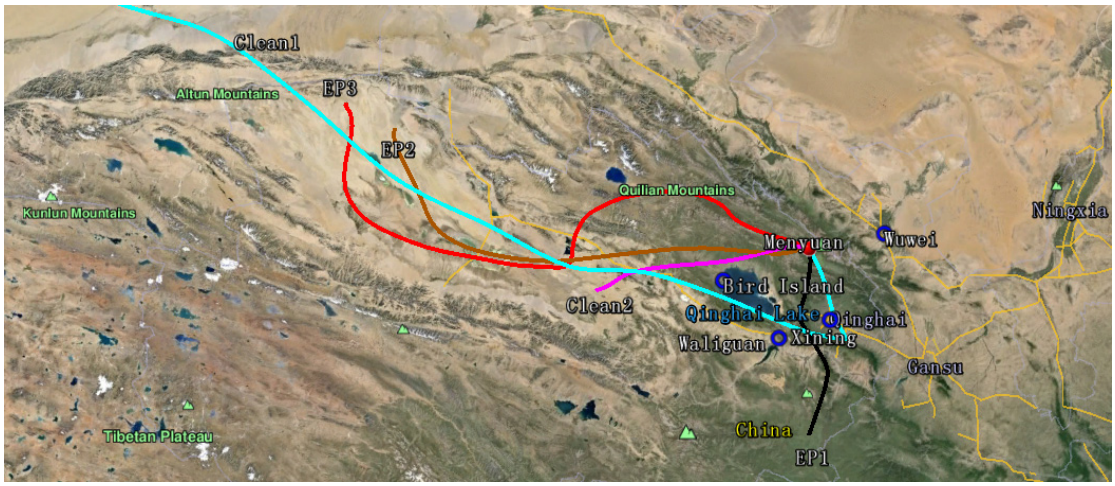

Fig. S3. The back trajectories during five episodes marked in Fig. 3. The time for each trajectory was 00:00 on 14 Sep. for Clean 1, 12:00 on 22 Sep. for Ep1, 00:00 on 27 Sep. for Ep2, 00:00 on 9 Oct. for Clean2, 00:00 on 14 Oct. for Ep3. The time is UTC time which is equal to Beijing time minus 8 hours.

It was a bit confusing seeing several comparisons in the text and figures with the other sites that are listed in the Supporting Information (SI) Table S1. Those sites are very far away from the sampling location and this paper is probably not intended to be a review of all aerosol composition measurements in China. It was also misleading that the Aerosol Chemical Speciation Monitor (ACSM) instrument is not sensitive to refractory material, which previously was shown to comprise over 60% of the $PM_{2.5}$ composition for a summertime study at the Bird Island site (Li et al., Tellus B, 2013). The Bird Island results are probably the most relevant published data for comparison, yet they were barely mentioned in the paper. It may be more appropriate to limit the other comparisons to a short, stand-alone section.

The main objective of Fig.1 and Table S1 was to have a better understanding of aerosol characteristics at the rural site on the Tibetan Plateau compared to other rural sites in Asia. As shown in Fig. 1, aerosol composition at the national background site in Menyuan was substantially different from that observed in eastern China and also that over the Pacific Ocean, indicating the different impacts of anthropogenic activities on regional background aerosols. Such information is important for readers to have a better knowledge of aerosol chemistry at various rural sites rather than one single site in East Asia. Although ACSM is insensitive to refractory materials, we focus on the comparisons of non-refractory submicron aerosol composition here. In addition, all the data in Fig. 1 and Table S1 were measured by Aerosol Mass Spectrometers, which can be directly compared to the results in our study. The study by Li et al. (2013) at the Bird Island site showed a large fraction of unknown material (61%) in $PM_{2.5}$. Without further analysis of the unknown materials, it is hard to tell that the unknown material was mainly mineral dust. There's also possibility that organic matter (OM) was underestimated when converting OC to OM with a low OM/OC ratio. Unfortunately, we didn't find the OM/OC ratio used in Li et al. (2013).

The Bird Island results were cited in the introduction but not compared in detail in the text. The reasons include: 1) Li et al. (2013) reported $PM_{2.5}$ composition rather than PM_1; 2) different techniques were used (offline filter sampling vs. online real-time measurements). For instance, filter sampling of

ammonium nitrate might have significant loss in summer; 3) the study by Li et al. (2013) was conducted in a different season; 4) Li et al. (2013) focus on the analysis of molecular markers in organic matter.

Section 3.1: As mentioned above, it would be useful to have a series of back trajectories for the site – wind-rose plots for the higher wind speed data. It was not clear where the winds were coming from at the various wind speeds. From the back trajectories presented in Figure S1, Clean1 appeared to be near Xining in the past 12 hours whereas Clean2 appeared to be only from desert. Why does the data with the back trajectory from near Xining appear "clean"? The back trajectories for Episodes(EP) 1, 2, and 3 of high mass concentrations were not presented. It would be helpful to see where the potential large sources are – desert, saline lakes, forest, populated areas (density map?), power plants, railroads, etc.

We thank the reviewer's comments. As shown in Fig. 3, there were no clear wind direction patterns during this study, which was also illustrated by the wind rose plot below (Fig. R1). The wind rose plot showed that high wind speeds were mainly from the north, the northeast, the south, and the southeast.

Although the back trajectory during clean 1 was near Xining, the trajectory height remained at more than 3000 m which was well above the elevation of Xining. This indicated that the air masses could be above the boundary layer height when passing through Xining, which explained the low aerosol loadings.

The typical trajectories during five episodes are now presented in supplementary, and some hot spots, like cities were marked. However, this study was not intending to investigate the impacts of deserts, saline lakes, and power plants to aerosol composition at the sampling site, these potential sources were not marked to avoid misleading readers. Still, the reviewer pointed out a good point, future studies, e.g., modeling work can be used to further investigate the sources and transport of aerosol particles on the Tibetan Plateau.

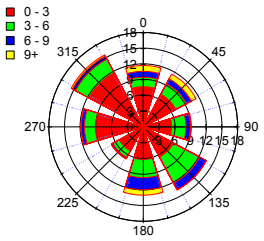

Fig. R1. Wind rose plot of for the entire campaign.

Section 3.2: The diurnal plots are difficult to interpret because all the data are combined and there was no common air mass history selected for this analysis. If biomass burning was a large local source, it should be removed from these plots. An indicator of time since emission could be determined from the fraction of total sulfur as sulfate or (sulfur from sulfate)/(sulfur from sulfur dioxide + sulfur from sulfate). This would only be relevant for sulfur sources and it is unclear that sulfur sources are coincident with other pollutants (for example, carbon monoxide or CO and BC) in the region.

We thank the reviewer's comments. The average diurnal plots for the entire study can eliminate the impacts of individual plumes and give the most important and common mechanisms driving the diurnal variations of aerosol species. Such an approach using diurnal plots to explore the formation mechanisms

and boundary layer dynamics has been widely used in the community of atmospheric chemistry. Although biomass burning was a large source of organic aerosol in this study, it won't change the overall diurnal patterns of aerosol species. For example, Fig. S4 shows the diurnal patterns of aerosol species after excluding biomass burning events which were remarkably similar to those with biomass burning events included. The diurnal variation of organics showed the largest difference as biomass burning aerosol was dominated by organic aerosol. Nevertheless, the diurnal cycle of OOA was exactly that of organics without biomass burning impacts, which is shown in Fig. 5 in the revised manuscript.

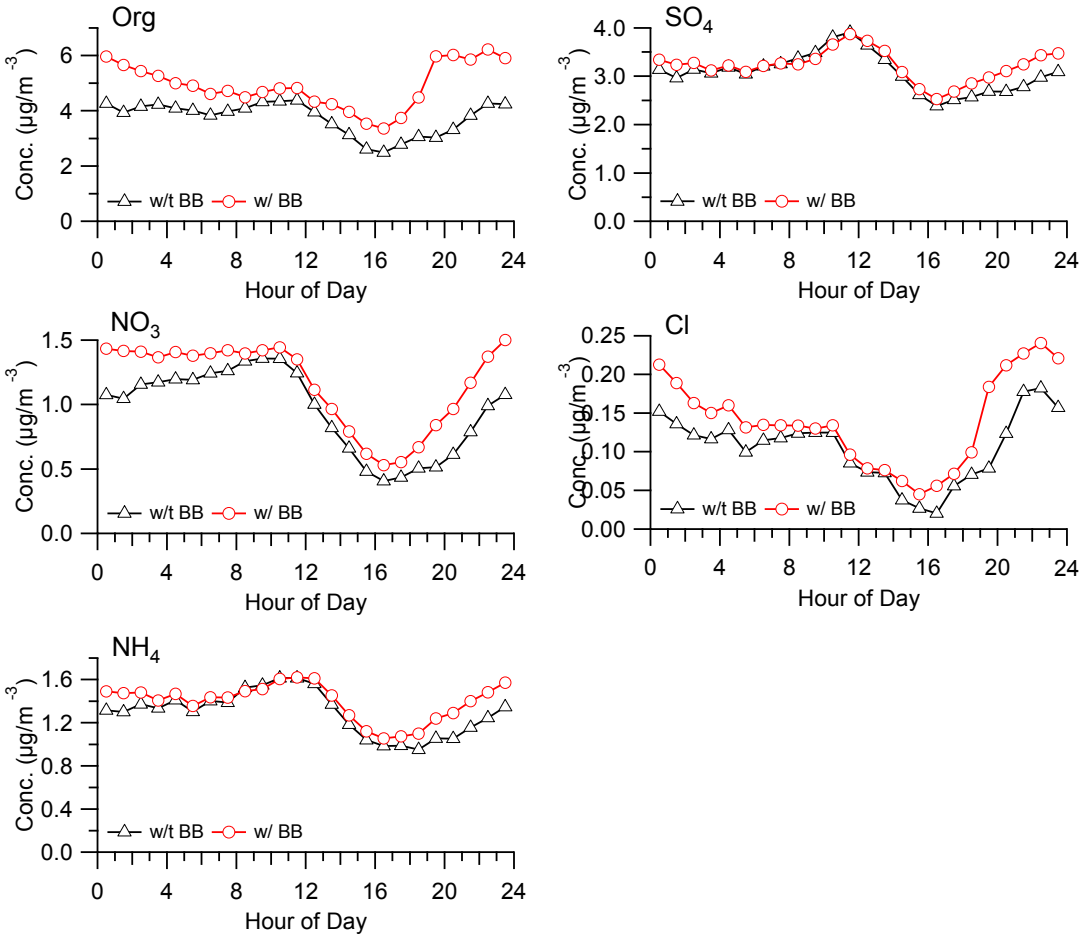

Fig. S4. Diurnal profiles of NR-PM_1 species with (w/) and without (w/t) biomass burning (BB) events.

The fraction of sulfur as sulfate in total sulfur, which is also known as sulfur oxidation ratio (SOR), can be used to indicate how much SO_2 is oxidized to sulfate (Fig. R2). The SOR is subject to multiple influences, for instance, gas-phase photochemical production and aqueous-phase processing. Considering that our sampling site is far away from point sources, it is difficult to use this ratio to evaluate the emission sources because of oxidation processing of SO_2 during the transport. But still, we observed some correlations between SO_2 and CO (see Fig. S5 for detail) except biomass burning events. It's likely that they were from the same sources. Modeling work is needed for further investigation which is beyond the scope of this study.

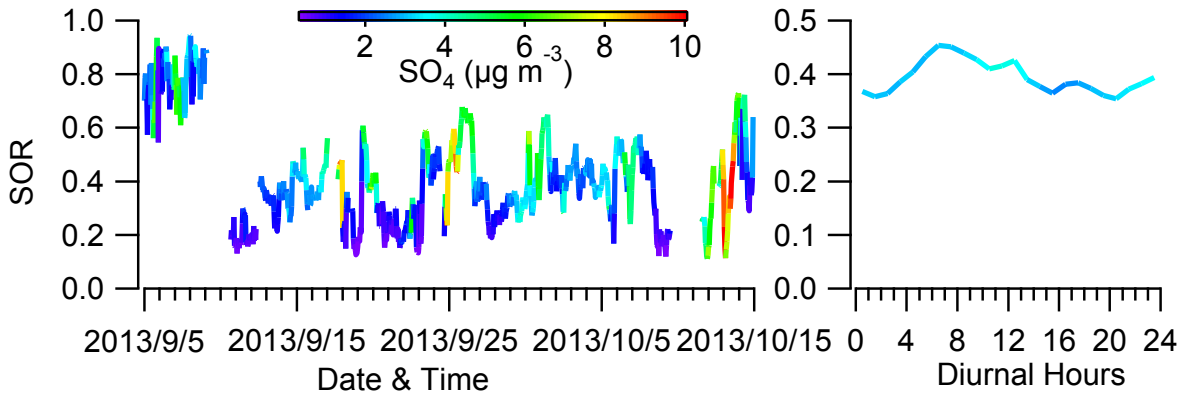

Fig. R2. The time series and diurnal variation of the fraction of S in total sulfur, which was calculated by (sulfur from sulfate)/(sulfur from sulfur dioxide + sulfur from sulfate).

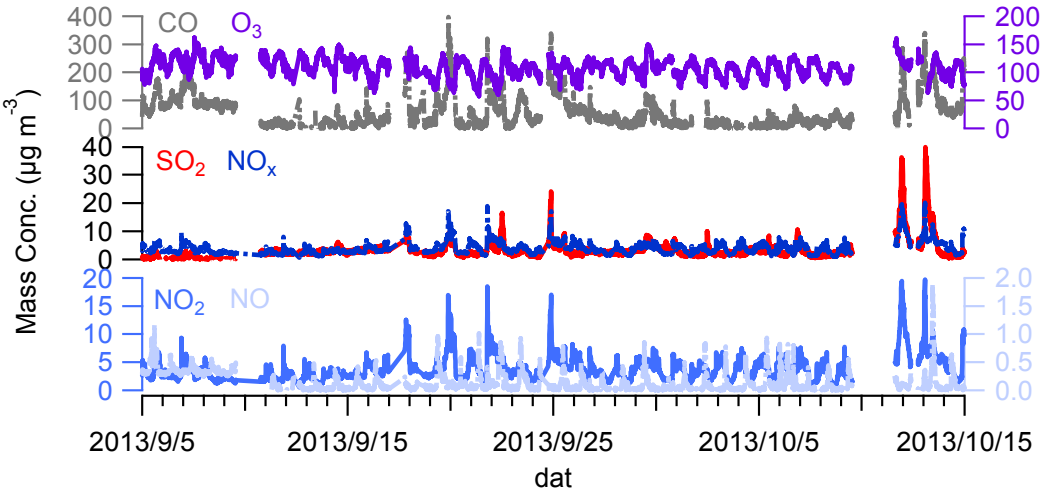

Fig. S5. Time series of gas phase species including CO, O_3, SO_2, NO_x, NO_2, NO during this study.

Section 3.3: It appears that biomass burning was a large local source of PM_1 during the study, however, this point was not made clear in this section.

The fresh and aged BBOA together accounted for 33% of the total OA, which is ~14% of PM_1. Following the reviewer's suggestion, we claimed the importance of BBOA as a local source in the revised manuscript, which is "The fresh and aged BBOA together accounted for 33% of the total OA suggesting that BBOA was a large local source of OA during the observational period."

Section 3.4: It would be helpful to know a bit more about the meteorology, wind speed and direction as a function of the time of day. Back trajectories would also be useful to interpret the data, especially since particle nucleation was previously observed at Mt. Waliguan for air masses originating from the western sector of that site. There is no physical basis for changes in the smallest particle diameter (Equation 2) to be correlated to bulk particle composition (Figure 9), especially since the size of particles measured by the ACSM is much larger than detected by the Scanning Mobility Particle Sizer (SMPS)

during new particle events. Suggest converting the growth rates from a diameter to volume unit for comparison and seeing if the volume increases match the mass increases.

Thank the reviewer's comments. The diurnal variations of temperature (T), relative humility (RH), wind speed (WS) and wind direct (WD) are shown in supplementary as Fig. S1. Different from Mt. Waliguan, we observed particle nucleation event for almost every day (~80% of the time). We agree with the reviewer that there was no direct relationship between bulk particle composition and particle growth at small sizes. The best way is to measure the chemical composition of nano particles which was unfortunately not available in this study. Therefore, we used the bulk composition change to demonstrate the potential role of aerosol species in particle growth. In fact, the particles with mobility diameter larger than 20 nm (approximately 30 nm in vacuum aerodynamic diameter) can be detected by the ACSM. The aerosol composition change could indicate, at least to a certain degree, their roles in particle growth.

The time series of SMPS volume concentration would be very similar to that of PM_1 since the estimated particle density was relatively constant (1.5 g cm^{-3}) and the SMPS mass (volume times density) agreed well with PM_1. Therefore, the diurnal cycles of particle volume during NPE and non-NPE would be similar to those of PM_1 in Fig. 8. No doubt, the volume increases would match the mass increases.

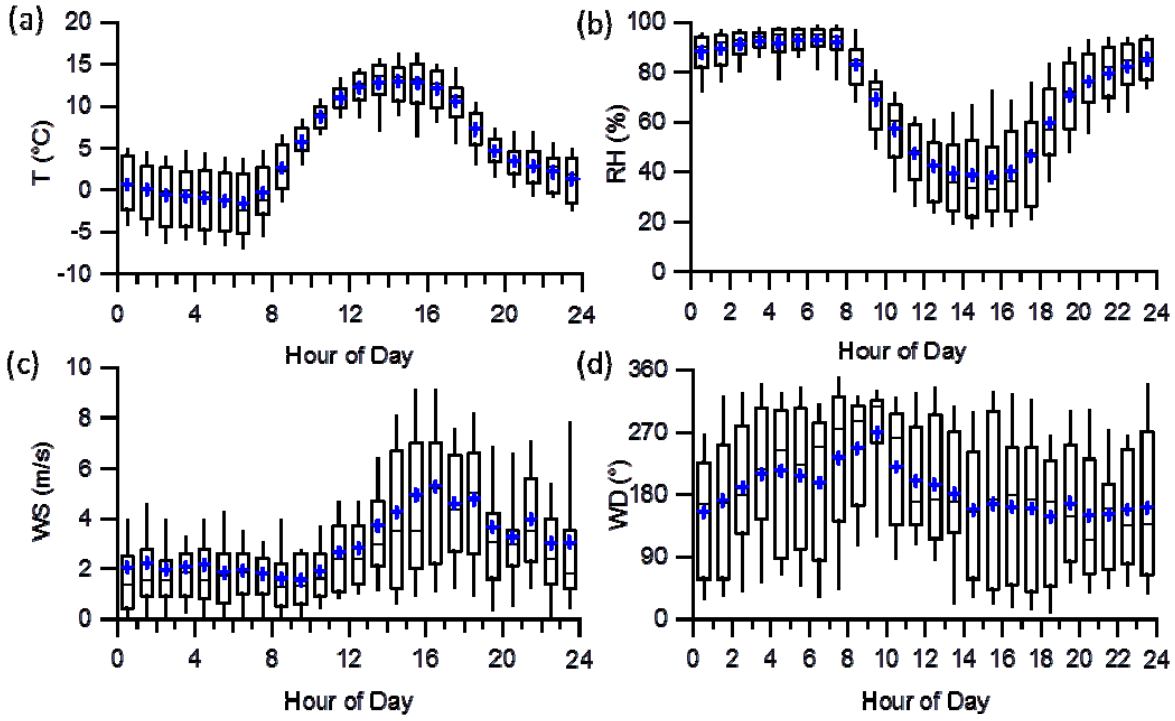

Fig. S1. The diurnal variation of meteorology including (a) temperature (T), (b) relative humility (RH), (c) wind speed (WS), and (d) wind direction (WD).

Other comments:

Title: change "in" to "on"

Changed.

Line 142: change “plotentilla” to “potentilla”

Changed.

Line 144: It seems that there were no other urban areas nearby. How big is Menyuan? Datong? Also mention the population of Xining. Are there railroads or power plants impacting the site? Note that the comparisons of city size and population need to be more quantitative, to be put into context with other locations around the world.

The area of Menyuan autonomous county is 6896 km^2 with a population of 155,800. Note that our sampling site is approximately 45 km from the town of Menyuan. In comparison, Datong autonomous county is 3090 km^2 with a population of 453,000. The population of Xining is 2,290,000 until 2013. The closest road near the sampling site is the national road G227. There are power plants in the city of Xining. As shown in our data, several SO_2 plumes might be impacted by the emissions from power plants. However, this study is not intending to investigate the impact of railway roads and power plants to aerosol chemistry at the national background site, therefore, we did not discuss such details in the text to avoid misleading the readers.

Following the reviewer’s suggestions, some quantitative information on the sampling site was added in the revised manuscript.

Line 146: define “few”

We thank the reviewer’s comment. During this study, we only saw sporadic vehicles on G227. Because we didn’t count the number vehicles passing through the national road G227, we cannot give the exact number here, so “few” was used here. The vehicle emissions could not make a large contribution to the aerosols at our sampling site because the concentration of traffic-related NO was very low, < 1 ppb for most of time (see Fig. S5 for detail).

Section 2.2: How high were the sampling inlets? How was black carbon measured?

The sampling height is approximately 2 m, and the particle residence time in the sampling tube is ~ 5 s. Black carbon was measured by an Aethalometer (AE31, Magee Scientific Corp.). Such information was added in section 2.2 in the revised manuscript.

Lines 205-207: Need to mention the particle size range that is transmitted into the ACSM.

ACSM measures aerosol particles in the size range of 10 nm – 1 μm (vacuum aerodynamic diameter), and SMPS measures aerosol particles in the size range of 12 – 478 nm. The size information on ACSM measurement was added in section 2.2.

Lines 273-279: These sentences imply that air is transported from Lanzhou to the site. Is that what was intended here? Perhaps it needs to be reworded.

Thank the reviewer’s comments. To avoid confusion, we deleted this sentence in the revised manuscript.

Section 3.2: This is the first place where the gas phase measurements are discussed. It would be helpful to have a time series of them in the SI.

Good suggestion. The time series of gas phase species including CO, O_3, SO_2, NO_x, NO_2, NO are now shown in the Fig. S5.

Line 369: change “rationale” to “rational”

Changed.

Line 403: change “bio-modal” to “bi-modal”

Corrected.

Line 448-449: How long would it take for urban air to get to the site?

It may take hours depending on wind speed and also the vertical convection.

Line 485: delete the word “ubiquitously”

Deleted.

Many of the figures do not include the units of measurements. Since the sampling site is at a high altitude, the units of everything should be converted to standard conditions (273.15 K temperature and 1013 hPa pressure). Units for gas phase data should be in mixing ratio (ppbv or pptv) instead of micrograms per cubic meter.

We thank the reviewer’s comments. The ambient mass concentrations can be easily converted to those under standard conditions using ideal gas law based on the measurements of pressure and temperature. However, we kept the ambient concentrations here to be consistent with previous studies in Qianghai e.g., (Li et al., 2013) and also the gas-phase species measurements. This was clearly stated in section 2.2 as “All the data are reported with ambient conditions at Beijing Standard Time”.

The concentrations of gaseous species can be reported either in mixing ratio with the units of ppbv or ppmv, or in micrograms per cubic meter that has been widely used in the community.

Figure 1: It should be noted that the pie-charts do not include dust and salts, which could be important for the total PM_1 at the National Background Site. Suggest making the inset satellite image larger than the pie-chart map (moving the pie chart map to SI). There should be a scale on the image, along with markers for other locations such as Bird Island, Mt. Waliguan, Xining, and Wuwei (another potentially significant “nearby” urban source). Consider making it a slightly larger scale to show the location of Lanzhou, too.

We thank the reviewer’s comments. Mineral dusts and salts have the dominant fraction in coarse particles and a small fraction in $PM_{2.5}$, for example, the water-soluble Ca^{2+} and Mg^{2+} together accounted for < 2% of $PM_{2.5}$ in Qianghai (Li et al., 2013). Considering that we measured PM_1 in this study, mineral dust and salts are expected to contribute a much smaller faction in PM_1. As a result, we don’t think that refractory dust and salts can make an important contribution to PM_1. More important, all the

comparisons in Fig. 1 are from AMS and BC measurements none of which included mineral dust and salts.

Fig. 1 is important for readers to understand the aerosol chemistry at the rural site on the Tibetan Plateau compared to other rural sites in Asia. It is of particular interest that aerosol composition at rural sites showed clear differences from the west to the east in Asia, which was strongly associated with the influences of anthropogenic activities. Therefore, we kept this figure in the revised manuscript. In addition, although previous measurements were conducted at various sites near Menyuan, e.g., Bird Island, Mt. Waliguan, Xining, and Wuwei, this study was not intended to compare with them since the measurements were different. To address the reviewer's comments, a large satellite image plot with the marked locations is given in Fig. S3

Figure 2: The correlation seems to change with time, where the SMPS is lower in the later part of the study by a larger amount than in the beginning. Is there a reason for this?

Right, we also noticed these differences. One of the reasons was likely due to the size differences between 12 – 478 nm and 478 nm – 1 μm during these periods. Unfortunately, we don't have the size measurements above 478 nm to investigate such differences.

Figure 3: It is difficult to see several traces on the figure, especially the wind direction, black carbon, and PM_1. Why are there gaps in the data? There is a clear diurnal pattern in wind speed. Is there a diurnal pattern in wind direction too?

We tried our best to make Fig. 3 clear to readers. The gaps in the Figure were caused by the unavailable BC data due to malfunction of the instrument. It seems that there was no clear pattern for wind direction (Fig. R1). As shown in Fig. S1, the wind direction varied largely throughout the day (see 25 – 75th percentiles).

Figure 4: It would be helpful in the caption to point out local sunrise and sunset. Note the legend should indicate that lines with symbols in Part (a) correspond to PM_1.

Good point, the time of sunrise and sunset were added in the caption in the revised manuscript. In addition, the legend for PM_1 was added in (a).

"Figure 4. Average diurnal cycles of (a) mass concentration; (b) mass fraction of PM_1 species; (c) ratios of aerosol species to CO, and (d) gaseous species. The local sunrise and sunset was around 7:00 and 19:00."

Figure 5: There should be tick marks on the top x-axis of Part (a) or perhaps a marker indicating where m/z 60 is located. It is difficult to distinguish the different colors in these plots.

The markers of *m/z* 60 and 73 were added in the figure. Because BBOA highly correlated with *m/z* 60, it's a bit difficult to distinguish these two species in the figure.

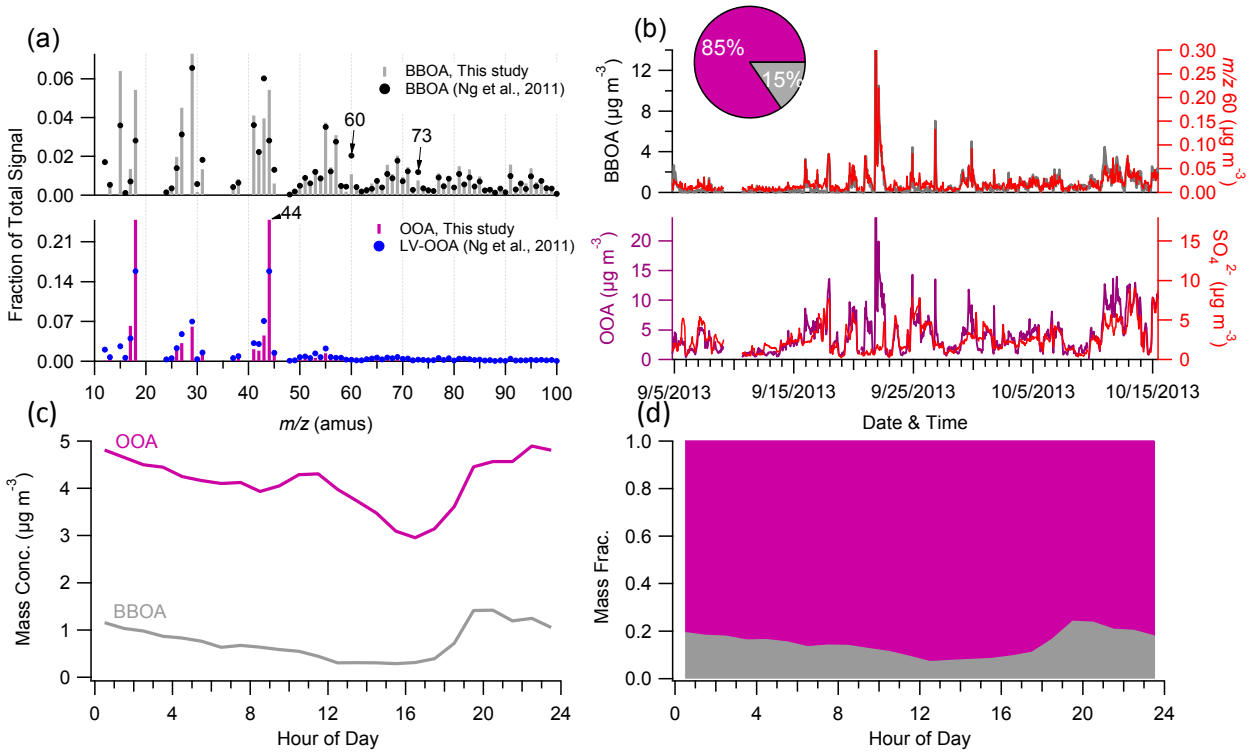

Fig. 5. (a) Mass spectra and (b) time series of mass concentrations of BBOA and OOA. (c) and (d) show the average diurnal cycles of BBOA and OOA. In addition, the standard average mass spectra of BBOA and OOA in Ng et al. (2011) are also shown in (a) for the comparison. The pie chart in (b) shows the average composition of OA for the entire study.

Figure 6: Should define in the caption what "post-processed OOA" means.

The post-processed OOA that is "OOA – SO_4× $[OOA/SO_4]_{NBB}$" was added in the caption.

Figure 7: For Part (b), need to label the y-axis and include text about the dotted lines in the caption. Should also note when it rained in Part (a) and the time of local sunrise in Part (d).

Fig. 7 was revised according to the reviewer's suggestions. Note that it's difficult to read if adding precipitation in (a). The readers can find precipitation information in Fig. 3.

Figure 8: Remove irrelevant plots (top mass concentration, mass fraction) or put into SI. Units for CO and PM_1/CO are missing. Again, note the time of local sunrise in the caption.

Thank the reviewer's comments. The diurnal plots of mass concentrations and mass fractions are important for readers to know the variations of aerosol species and composition during NPE and non-NPE events. Therefore we kept them in the revised manuscript. The unit of CO, and the sunrise time were added. Note that PM_1/CO has no unit since both PM_1 and CO were reported in μg m^{-3}.

Figure 9: The bottom plot in Part (a) is probably not relevant and could be removed. Suggest creating a new plot for Part (b) with growth rate in units of volume change per unit time and aerosol mass change (the difference in mass normalized to CO) per unit time. Still may not be correlated if the size ranges are not overlapping.

We thank the reviewer's comments. Fig. 9a is important for readers to know the variations of particle growth rates and also chemical composition, thus we kept it in the revised manuscript. The time series of SMPS volume concentration would be very similar to that of PM_1 since the estimated particle density was relatively constant (1.5 g cm^{-3}) and the SMPS mass agreed well with PM_1. Therefore, the diurnal cycles of particle volume during NPE and non-NPE would be similar to those of PM_1 in Fig. 8. The volume concentration would show decreases during NPE. Even considering the dilution by planetary boundary layer height using CO, the variation of the volume concentration would be also small (see Fig. 4c for PM_1/CO). In addition, the diurnal variation of OOA was similar to most of aerosol species in this study. As a result, we don't think it can tell us much information by linking particle volume with OOA. Here, we focus on the relationship between the growth of particle sizes and aerosol composition. Such an approach was also used in many previous studies on new particle formation. However, we agree with the reviewer that our understanding of NPE and aerosol composition were still limited because no size-resolved composition was available in this study. Future studies are absolutely needed for further investigations.

Table S1: Make headers match the site location names on the map form Figure 1.

Following the reviewer's suggestion, we corrected the headers of Table S1.

"Table S1 A summary of mass concentration and composition of PM_1 species measured by AMS at different locations in East Asia."

Location		Okinawa Japan	Fukue Japan	Jeju Korea	Jiaxing Shanghai	Changdao Island	Mount.Tai	Kaiping Shenzhen	Lanzhou
Time		10/3/2003 10/28/2003	3/20/2003 4/18/2003	4/13/2001 4/30/2001	6/29/2013 7/15/2013	3/21/2011 4/24/2011	2011	10/12/2008 11/18/2008	7/11/2012 8/7/2012
Org	Mass	3.1	5.0	3.5	10.6	13.4	11.2	11.2	11.5
	Frac.	21.4	41.7	40.7	32.1	28.8	32.6	33.9	47
SO_4	Mass	9.2	4.8	3.1	8.2	8.3	9.2	11.1	3.9
	Frac.	63.4	40.0	36.0	25.2	17.8	26.7	33.6	16
NO_3	Mass	0.19	0.56	0.51	5.9	12.2	7.2	3.5	2.5
	Frac.	1.3	4.7	5.9	18.0	26.1	20.9	10.7	10
NH_4	Mass	1.9	1.6	1.5	4.2	6.5	5.8	4.6	2.7
	Frac.	13.1	13.3	17.4	12.6	13.9	16.9	14.0	11
Chl	Mass.	0.06	0.07		1.0	1.3	0.95	0.36	1.0

	Frac.	0.4	0.6		3.0	2.8	2.8	1.1	4
BC	Mass				3.0	2.5		2.2	2.9
	Frac.				9.1	5.4		6.7	12
NR-PM_1		14.5	12.0	8.6	29.9	44.1	34.4	30.8	21.6
PM_1					32.9	46.6		33.1	24.5
References		(Zhang et al., 2007)	(Takami et al., 2005)	(Topping et al., 2004)	(Huang et al., 2013)	(Hu et al., 2013)	(Zhang et al., 2014a)	(Huang et al., 2011)	(Xu et al., 2014)

Figure S2: Add the outline of Qinghai Lake and the locations of Qilian Shan Station, Bird Island, Mt. Waliguan, and Xining, Maybe Wuwei. Is the black curve on the bottom plot indicating the ground level? Please note that in the caption. Also add the time difference between UTC and the sampling site.

Thank the reviewer's suggestions. A new figure with the back trajectories of five episodes is presented in supplementary. The locations of various sites mentioned by the reviewer were marked in the figure, and the back trajectory time was also included in the caption.

Response to Reviewer #2

The paper entitled of "Chemical characterization of submicron aerosol and particle growth events at a national background site (3295 m a.s.l) in the Tibetan Plateau" present the first high-time resolution chemical composition measurement in the Tibetan Plateau where the chemical composition and distribution are important factors for evaluating the climate forcing of aerosol. PMF analysis is applied on organic mass spectra and obtains two factors and the results show biomass burning emitted aerosol is an important source for primary and secondary OA. In addition, at this remote area, the paper also shows new particle formation (NPF) events are an important chemical process and aerosol source. The topic of this paper is interesting and suitable for publication in ACP. I agree this paper for publication after revising following comments and suggestions below.

We thank the reviewer's positive comments.

Specific comments:

Section 2.1: add several sentences for describing the meteorological conditions of study period, such as air temperature, precipitation, and wind condition.

Following the reviewer's suggestions, we expanded the discussions on meteorological conditions in the revised the manuscript.

In this study, ambient temperature averaged 4.9 ^{o}C (-8.7 - 17.9 ^{o}C) and wind speed varied largely with an average value of 3 m s^{-1}. In addition, several precipitation events were also observed, particularly during the first half period of this study (Fig. 3).

Section 2.2: What is the environment condition for instruments? What is the length of inlet and the size of critical orifice? Because the particle loss can be a problem at the high elevation sampling site, so these issue should be considered. In addition, does the SMPS work well at such high elevation site?

All the instruments were placed in an air-conditioned room with the temperature maintaining at ~23^{o}C.

The length of the sampling line (1/2 inch stainless steel) is approximately 2 m. The residence time of aerosol particles in the sampling tube is estimated to be ~ 5 s and the size of critical orifice for ACSM inlet is 100 μm. Therefore, the particle loss for ACSM measurements should be small. The butanol-based SMPS worked well at such a high elevation site (3295 m). This is also supported by the good agreements between ACSM and SMPS (Fig. 2). We agree with the reviewer that SMPS might have problems at a higher elevation site due to the limitation of vapor pressure of butanol.

Section 3.1, p13524, line9-14: the chemical composition of PM1 during the two clean periods may reflect the aerosol composition at the free troposphere which the contribution of sulfate were much higher than those non-clean periods, can the author give some explanations for this phenomenon.

There's possibility that the aerosol composition during clean periods were affected by free troposphere. According to previous studies (Zhang et al., 2014b), the nighttime would be the period with the largest influence from free troposphere when planetary boundary layer (PBL) height is low. Considering both clean period and pollution events generally lasted more than one day, both of them could be affected by the free troposphere. Unfortunately, we were unable to quantify the chemical composition of aerosol from free troposphere based on the measurements in this study.

However, we noticed that the chemical composition during clean periods showed much lower contribution of nitrate that was dominantly from the oxidation of anthropogenic NO_x. Therefore, the higher sulfate and lower nitrate during clean periods might suggest that the air masses during clean periods were either from a longer transport when ammonium nitrate was deposited or evaporated due to dilution processes, or from less anthropogenic influenced regions with low nitrate.

Following the reviewer's suggestion, we expanded the interpretation of the chemical differences between clean periods and pollution episodes.

"We also noticed that the two clean periods showed overall higher contribution of sulfate and lower contribution of nitrate compared to the three pollution episodes. The possible reasons were likely due to that the air masses during clean periods were either from a longer transport when ammonium nitrate was deposited or evaporated due to dilution processes, or from less anthropogenic influenced regions with low NO_x emissions."

Section 3.1, P13524 line 25 to P13525 line 4: As illustrated at section 3.4, sulfate can be from the new particle formation (NPF) as sulfuric acid is an important component for NPF. Acidic PM1 particle was also observed at QSS at the Qilianshan Mountain at the northeastern TP which use filter measurement by MOUDI.

It's a good point. We added such an explanation in the revised manuscript. "Also note that the newly formed sulfate particles during the frequent NPF events might also have played a role". In addition, the work conducted at the Qilainshan Mountain (Xu et al., 2015a) was cited.

Section 3.3: Are the diurnal pattern of these two factors evidently? It is better to show diurnal variations in the Fig.5 which is useful to support the results of PMF analysis. In addition, it is interesting that the OOA is highly oxidized, but the possible explanations are not given by the authors. The aqueous processes may be an important factor for this highly oxidized OOA because the extremely high RH (seems more than 95% in Fig.1) during night-time every day.

Yes, the diurnal patterns of OOA and BBOA were evident (Fig. 5). While OOA showed similar diurnal variations to that of PM_1, BBOA was characterized by higher concentration at nighttime. Following the reviewer's suggestions, the diurnal patterns of OOA and BBOA were added in Fig. 5 in the revised manuscript, and the related discussions were expanded in section 3.3.

OOA is highly oxidized suggesting that OOA was well processed at the national background site. As the reviewer mentioned that aqueous-phase processing at nighttime might also play a role. Such explanations were added in the revised manuscript.

Section 3.4: It is not easy to say which species is the major contribution for NPF using the whole size range aerosol composition. But it is not other better way to get the small size range chemical composition using ACSM. One suggestion is to get some information from single particle composition if these data are available.

This is a good suggestion. Unfortunately, the single particle composition data was not available in this study.

Technical comments:

P13517, line 21: ~200000 km^2 → ~2000000 km^2

Corrected.

P13525, line 20: decreases → decreased to

Changed.

P13526, line 22: large plumes → large peaks

Changed.

P13527, line 25: Figs. 5b and 6 → Fig. 5b and 6; the different correlation → the weak correlation

Changed.

P13528, line 10: rationale → rasionable

We changed "rationale" to "rational".

P13528, line 25: check the number of 3.9 μg m^{-3}

Thank the reviewer's carefulness. It was corrected as "0.82 (± 2.65) μg m^{-3}"

P13530, line 15-19: "the results …… this period" is a repeat information.

It was deleted in the revised manuscript.

P13531, line7: change → variation

Changed.

P13532, line2: Y. M. Zhang et al. (2011) → Zhang et al. (2011)

Corrected.

P13532: line 10: 5 September or 4 September

Thank the reviewer's carefulness. It was 5 September. All the date was corrected in the revised manuscript.

References:

Hennigan, C. J., Miracolo, M. A., Engelhart, G. J., May, A. A., Presto, A. A., Lee, T., Sullivan, A. P., McMeeking, G. R., Coe, H., Wold, C. E., Hao, W. M., Gilman, J. B., Kuster, W. C., de Gouw, J., Schichtel, B. A., Collett, J. L., Kreidenweis, S. M., and Robinson, A. L.: Chemical and physical transformations of organic aerosol from the photo-oxidation of open biomass burning emissions in an environmental chamber, Atmospheric Chemistry and Physics, 11, 7669-7686, 10.5194/acp-11-7669-2011, 2011.

Hu, W. W., Hu, M., Yuan, B., Jimenez, J. L., Tang, Q., Peng, J. F., Hu, W., Shao, M., Wang, M., Zeng, L. M., Wu, Y. S., Gong, Z. H., Huang, X. F., and He, L. Y.: Insights on organic aerosol aging and the influence of coal combustion at a regional receptor site of central eastern China, Atmospheric Chemistry and Physics, 13, 10095-10112, 10.5194/acp-13-10095-2013, 2013.

Huang, X.-F., Xue, L., Tian, X.-D., Shao, W.-W., Sun, T.-L., Gong, Z.-H., Ju, W.-W., Jiang, B., Hu, M., and He, L.-Y.: Highly time-resolved carbonaceous aerosol characterization in Yangtze River Delta of China: composition, mixing state and secondary formation, Atmos. Environ., 64, 200 - 207, 10.1016/j.atmosenv.2012.09.059, 2013.

Huang, X. F., He, L. Y., Hu, M., Canagaratna, M. R., Kroll, J. H., Ng, N. L., Zhang, Y. H., Lin, Y., Xue, L., Sun, T. L., Liu, X. G., Shao, M., Jayne, J. T., and Worsnop, D. R.: Characterization of submicron aerosols at a rural site in Pearl River Delta of China using an Aerodyne High-Resolution Aerosol Mass Spectrometer, Atmospheric Chemistry and Physics, 11, 1865-1877, 10.5194/acp-11-1865-2011, 2011.

Li, J. J., Wang, G. H., Wang, X. M., Cao, J. J., Sun, T., Cheng, C. L., Meng, J. J., Hu, T. F., and Liu, S. X.: Abundance, composition and source of atmospheric PM 2.5 at a remote site in the Tibetan Plateau, China, Tellus B, 65, 2013.

Takami, A., Miyoshi, T., Shimono, A., and Hatakeyama, S.: Chemical composition of fine aerosol measured by AMS at Fukue Island, Japan during APEX period, Atmos. Environ., 39, 4913-4924, 2005.

Topping, D., Coe, H., McFiggans, G., Burgess, R., Allan, J., Alfarra, M. R., Bower, K., Choularton, T. W., Decesari, S., and Facchini, M. C.: Aerosol chemical characteristics from sampling conducted on the Island of Jeju, Korea during ACE Asia, Atmospheric Environment, 38, 2111-2123, 10.1016/j.atmosenv.2004.01.022, 2004.

Xu, J., Zhang, Q., Chen, M., Ge, X., Ren, J., and Qin, D.: Chemical composition, sources, and processes of urban aerosols during summertime in northwest China: insights from high-resolution aerosol mass spectrometry, Atmos. Chem. Phys., 14, 12593-12611, 10.5194/acp-14-12593-2014, 2014.

Xu, J. Z., Zhang, Q., Wang, Z. B., Yu, G. M., Ge, X. L., and Qin, X.: Chemical composition and size distribution of summertime PM2.5 at a high altitude remote location in the northeast of the Qinghai–Xizang (Tibet) Plateau: insights into aerosol sources and processing in free troposphere, Atmos. Chem. Phys., 15, 5069-5081, 10.5194/acp-15-5069-2015, 2015a.

Xu, J. Z., Zhang, Q., Wang, Z. B., Yu, G. M., Ge, X. L., and Qin, X.: Chemical composition and size distribution of summertime PM_{2.5} at a high altitude remote location in the northeast of the Qinghai–Xizang (Tibet) Plateau: insights into aerosol sources and processing in free troposphere, Atmospheric Chemistry and Physics, 15, 5069-5081, 10.5194/acp-15-5069-2015, 2015b.

Zhang, Q., Jimenez, J. L., Canagaratna, M. R., Allan, J. D., Coe, H., Ulbrich, I., Alfarra, M. R., Takami, A., Middlebrook, A. M., Sun, Y. L., Dzepina, K., Dunlea, E., Docherty, K., DeCarlo, P. F., Salcedo, D., Onasch, T., Jayne, J. T., Miyoshi, T., Shimono, A., Hatakeyama, S., Takegawa, N., Kondo, Y., Schneider, J., Drewnick, F., Borrmann, S., Weimer, S., Demerjian, K., Williams, P., Bower, K., Bahreini, R., Cottrell, L., Griffin, R. J., Rautiainen, J., Sun, J. Y., Zhang, Y. M., and Worsnop, D. R.: Ubiquity and dominance of oxygenated species in organic aerosols in anthropogenically-influenced Northern Hemisphere midlatitudes, Geophysical Research Letters, 34, L13801

10.1029/2007gl029979, 2007.
Zhang, Y. M., Zhang, X. Y., Sun, J. Y., Hu, G. Y., Shen, X. J., Wang, Y. Q., Wang, T. T., Wang, D. Z., and Zhao, Y.: Chemical composition and mass size distribution of PM₁ at an elevated site in central east China, Atmospheric Chemistry and Physics, 14, 12237-12249, 10.5194/acp-14-12237-2014, 2014a.
Zhang, Y. M., Zhang, X. Y., Sun, J. Y., Hu, G. Y., Shen, X. J., Wang, Y. Q., Wang, T. T., Wang, D. Z., and Zhao, Y.: Chemical composition and mass size distribution of PM1 at an elevated site in central east China, Atmos. Chem. Phys., 14, 12237-12249, 10.5194/acp-14-12237-2014, 2014b.

Chemical Characterization of Submicron Aerosol and Particle Growth Events at a National Background Site (3295 m a.s.l.) on~~in~~ the Tibetan Plateau

W. Du[1,2], Y. L. Sun[1,*], Y. S. Xu[3], Q. Jiang[1], Q. Q. Wang[1], W. Yang[3], F. Wang[3], Z. P. Bai[3], X. D. Zhao[4], and Y. C. Yang[2]

[1]State Key Laboratory of Atmospheric Boundary Layer Physics and Atmospheric Chemistry, Institute of Atmospheric Physics, Chinese Academy of Sciences, Beijing 100029, China

[2]Department of Resources and Environment, Air Environmental Modeling and Pollution Controlling Key Laboratory of Sichuan Higher Education Institutes, Chengdu University of Information Technology, Chengdu 610225, China

[3]Chinese Research Academy of Environmental Sciences, Beijing 100012, China

[4]National Station for Background Atmospheric Monitoring, Menyuan, Qinghai 810000, China

*Correspondence to: Y. L. Sun (sunyele@mail.iap.ac.cn)

Abstract

Atmospheric aerosols exert highly uncertain impacts on radiative forcing and also have detrimental effects on human health. While aerosol particles are widely characterized in megacities in China, aerosol composition, sources and particle growth in rural areas in the Tibetan Plateau remain less understood. Here we present the results from an autumn study that was conducted from 5 September to 15 October 2013 at a national background monitoring station (3295 m a.s.l.) in the Tibetan Plateau. The submicron aerosol composition and particle number size distributions were measured in ~~-~~situ with an Aerodyne Aerosol Chemical Speciation Monitor (ACSM) and a Scanning Mobility Particle Sizer (SMPS). The average mass concentration of submicron aerosol (PM_1) is 11.4~~9~~ μg m^{-3} (range: 1.0 - 78.4 μg m^{-3}) for the entire study, which is much lower than those observed at urban and rural sites in eastern China. Organics dominated PM_1 on average accounting for 43%, followed by sulfate (28%) and ammonium~~nitrate~~ (11~~0~~%). Positive matrix factorization analysis of ACSM organic aerosol (OA) mass spectra identified an oxygenated OA (OOA) and a biomass burning OA (BBOA). The OOA dominated OA composition accounting for 85% on average, 17% of which was inferred from aged BBOA. The BBOA contributed a considerable fraction of OA (15%) due to the burning of cow dung and straws in September. New particle formation and growth events were frequently observed (80% of time) throughout the study. The average particle growth rate is 2.0 nm hr^{-1} (range: 0.8 – 3.2 nm hr^{-1}). By linking the evolution of particle number size distribution to aerosol composition, we found an elevated contribution of organics during particle growth periods and also a positive relationship between the growth rate and the fraction of OOA in OA, which potentially indicates an important role of organics in particle growth in the Tibetan Plateau.

Keywords

Tibetan Plateau; ACSM; Submicron Aerosol; OOA; BBOA; Particle Growth

1 Introduction

High concentration of atmosphere aerosol associated with the rapid economic growth, urbanization and industrialization has become a major environmental concern in China. Aerosol particles especially fine particles ($PM_{2.5}$) have large impacts on human health, natural ecosystem, weather and climate, radiative balance and the self-purification capacity of troposphere (Jacobson, 2001; Tie and Cao, 2009). As a result, a large number of studies have been conducted to investigate the sources, chemical and physical properties, and evolution processes of aerosol particles at urban and rural sites in China during the last decade (Cao et al., 2007; Wu et al., 2007; He et al., 2011; Gong et al., 2012; Huang et al., 2012; Huang et al., 2013; Sun et al., 2013). The results showed that fine particles are mainly composed of organics, sulfate, nitrate, ammonium, mineral dust, and black carbon. The sources of organic aerosol (OA) were also characterized and various OA factors from distinct sources were identified including primary OA (POA), e.g., hydrocarbon-like OA (HOA), cooking OA (COA), biomass burning OA (BBOA) and coal combustion OA (CCOA), and secondary OA (SOA), e.g., semi-volatile oxygenated OA (SV-OOA) and low volatility OOA (LV-OOA) (Huang et al., 2010; Sun et al., 2010; He et al., 2011; Huang et al., 2011; Xu et al., 2014a). While previous studies significantly improve our understanding on the sources and chemical properties of aerosol particles, they were mainly conducted in developed areas in China, including Beijing-Tianjin-Hebei, Pearl River Delta and Yangtze River Delta.

The Tibetan Plateau (~ 2,000,000 square kilometers) is the highest plateau in the world with an average altitude of over 4000 meters above sea level. The Tibetan Plateau is an ideal location for charactering rural and regional background aerosol due to minor influences of anthropogenic activities. However, chemical characterization of aerosol particles in the Tibetan Plateau is rather limited, and therefore their sources, properties, and evolution processes are poorly known. Cong et al. (2015) reported the seasonal variations of various aerosol components including carbonaceous species and water-soluble ionic species on the south edge of the Tibetan Plateau. Sulfate was found to dominate the total ionic mass (25%) followed by nitrate. In addition, most

aerosol species showed pronounced season variations in the pre-monsoon period due to biomass burning impacts from India and Nepal. Zhao et al. (2013) also characterized the chemical composition and sources of total suspended particulate (TSP) at Lulang on the southeastern TP based on one year measurement. Similar seasonal variations with higher concentrations during pre-monsoon were observed. The back trajectory analysis showed evident transport of air pollutants from south Asia to the TP. The analysis of size-segregated aerosol samples collected at a remote site in the inland Tibetan Plateau during 2012 further confirmed the high concentrations of organic carbon (OC) and elemental carbon (EC) during the pre-monsoon period (Wan et al., 2015), although their concentrations in PM_1 (2.38 and 0.08 μg m^{-3}, respectively) were much lower than those reported in eastern China. Most studies above were conducted in the southeastern Tibetan Plateau. Comparatively, aerosol particles showed quite different behavior in the northeastern Tibetan Plateau. Li et al. (2013) investigated the sources and chemical composition of fine particles collected at a remote site (Qinghai Lake) in the summer of 2010 in the Tibetan Plateau. The average $PM_{2.5}$ concentration was 22±13 μg m^{-3} with sulfate and carbonaceous aerosol being the two major species. Xu et al. (2014b) conducted a year-long measurement of $PM_{2.5}$ composition at the Qilian Shan Station, The annual average concentration of $PM_{2.5}$ was 9.5 ± 5.4 μg m^{-3} with water-soluble ions accounting for 39% of total mass. Water-soluble ions were dominated by sulfate (39%) and showed pronounced seasonal variations. The aerosol composition, size distributions, and back trajectory analysis together indicated a mixed impact of both mineral dust from arid areas of northwest China and anthropogenic emissions from urban areas. However, previous extensive efforts to characterize the chemical properties of aerosol particles in the Tibetan Plateau heavily rely on filter measurements with the duration ranging from days to weeks, real-time measurement of aerosol particle composition is still very limited. A recent study by Xu et al. (2014a) deployed a high-resolution time-of-flight aerosol mass spectrometer (HR-ToF-AMS) at an urban site in Lanzhou in northwest China. The submicron aerosol in the city was dominated by organic aerosol (47%) with a large contribution from local traffic and

cooking emissions (40%). To our knowledge, there is no such real-time measurement of aerosol particle composition with aerosol mass spectrometer at rural sites in the Tibetan Plateau yet.

The study of new particle formation and growth events in the Tibetan Plateau is also relatively new. Since 2004, a number of studies have been conducted to investigate the new particle formation (NPF) and particle growth events in various environments in China (Wu et al., 2007; Wiedensohler et al., 2009; Yue et al., 2010; Zhang et al., 2011b; Wang et al., 2013a; Wang et al., 2013b). The NPF events were frequently observed in urban cities, rural sites, coastal regions, and mountain sites. Sulfuric acid was found to play a dominant role in both NPF and subsequent particle growth, while organics makes an important contributor to particle growth (Yue et al., 2010). The particle growth rates varied largely depending on sites and days, yet generally fell within 1 – 20 nm hr^{-1}. Kivekas et al. (2009) conducted a long-term measurement of particle number size distributions at Waliguan, a regional background site located approximately 140 km southwest of our sampling site. The annual average particle number concentration was found to be higher than other rural sites in the world. Despite this, the particle growth and its relationship to chemical species in the Tibetan Plateau are rarely investigated and remain poorly understood.

In this study, an Aerodyne Aerosol Chemical Speciation Monitor (ACSM) was first deployed at a national background monitoring site (Menyuan, Qinghai) in the Tibetan Plateau for the real-time characterization of submicron aerosol composition including organics, sulfate, nitrate, ammonium, and chloride from 54 September to 15 October, 2013. Collocated measurements including black carbon and particle number size distributions were also conducted at the same site. Here we report the aerosol composition and variations of submicron aerosols and investigate the sources of organic aerosol with positive matrix factorization (PMF). In addition, the particle growth events are also characterized and the roles of chemical species in particle growth are elucidated.

2 Experimental method

2.1 Sampling site

The sampling site, i.e., the national atmospheric background monitoring station (NBS) (37º36´30"N, 101º15´26"E, 3295 m a.s.l.) is located on the Daban Mountain in Menyuan, Qinghai province (Fig. 1). The sampling site is characterized by a typical Plateau continental climate with a pleasantly cool and short summer, and a long cold winter. The annual average temperature is -1~-2º C, and the precipitation is 426 - 860 mm. In this study, ambient temperature averaged 4.9 ºC (-8.7 - 17.9º C) and wind speed varied largely with an average value of 3 m s^{-1}. In addition, several precipitation events were also observed, particularly during the first half period of this study (Fig. 3). The diurnal profiles of meteorological conditions including temperature, relative humidity, wind speed, and wind direction are shown in Fig. S1. The sampling site is relatively pristine with most areas covered by typical Tibetan Plateau plants, e.g., potentilla~~plotentilla~~ fruticosa and kobresia etc. There are no strong local anthropogenic source emissions in this area (~ 741 km^2 with a population of ~2000) except occasional biomass burning events that were observed during this study. The capital city Xining of Qinghai province with a population of 2,290,000 is approximately 160 km south of the sampling site which is connected by a national road G227 with few traffic vehicles.–

2.2 Instrumentation

The field measurements were conducted from 54 September to 15 October 2013. All the instruments were placed in an air-conditioned room with the temperature maintaining at ~23 ºC. The chemical compositions of non-refractory submicron aerosol (NR-PM_1) species including organics (Org), sulfate (SO_4), nitrate (NO_3), ammonium (NH_4) and chloride (Cl) were measured *in-situ* by an Aerodyne ACSM (Ng et al., 2011b). A $PM_{2.5}$ cyclone (Model: URG-2000-30ED) was supplied in front of the sampling line to remove coarse particles larger than 2.5 µm. The ambient air was drawn inside the room through a 1/2 inch (outer diameter) stainless steel tube using an external pump (flow rate is ~3 L min^{-1}). The sampling height is approximately 2 m, and the particle residence time in the sampling tube is ~ 5s. A silica gel diffusion dryer was then used to dry aerosol particles before sampling into

the ACSM. After passing through a 100 μm critical orifice, ~~the aerodynamic lens,~~ aerosol particles between 30 nm – 1 μm are focused into a narrow particle beam via the aerodynamic lens in the vacuum chamber, and then flash vaporized and ionized at a heated surface (~600^{o}C). The positive ions generated are finally analyzed by a commercial quadrupole mass spectrometer. In this study, the mass spectrometer of ACSM was operated at a scanning rate of 500 ms amu^{-1} from *m/z* 10 to 150. The time resolution is approximately 15 min by alternating 6 cycles between the ambient air and particle-free air. The detailed operation of ACSM has been given in Sun et al.(2012).

In addition to ACSM measurements, a Scanning Mobility Particle Sizer (TSI, 3936) equipped with a long Differential Mobility Analyzer (DMA) was simultaneously operated to measure the particle number size distributions between 11.8 nm – 478.3 nm at a time resolution of 5 min. Other collocated species includ~~ing~~ed CO, O_3, NO_x, and SO_2 ~~were also measured~~ by various gas analyzers from Thermo Scientific and black carbon (BC) by an Aethalometer (AE31, Magee Scientific Corp.). The meteorological parameters, e.g., temperature, relative humidity, pressure, visibility, precipitation, wind speed and wind direct were also recorded at the same site. All the data are reported with ambient conditions at Beijing Standard Time.

2.3 Data analysis

The ACSM data were analyzed within Igor Pro (WaveMetrics, Inc., Oregon USA) using the standard ACSM data analysis software (v.1.5.3.0). The mass concentrations and chemical composition of NR-PM_1 species were obtained using the default relative ionization efficiency (RIE) that is 1.4, 1.2, 1.1 and 1.3 for organics, sulfate, nitrate and chloride, respectively, except ammonium (6.5) that was derived from pure ammonium nitrate during ionization efficiency (IE) calibration. A collection efficiency (CE) of 0.5 was used to account for the incomplete detection of aerosol species (Matthew et al., 2008; Middlebrook et al., 2012) because aerosol particles were dry and only slightly acidic, and also the mass fraction of ammonium nitrate is not high enough to affect CE significantly.

The sources of organic aerosol were investigated by performing Positive Matrix Factorization (PMF2.exe, v 4.2) on ACSM OA mass spectra (Paatero and Tapper, 1994; Ulbrich et al., 2009). PMF is a standard multivariate factor analysis model broadly used in the field of air pollution source apportionment. The detailed PMF analysis of organic aerosol from AMS measurements, including error matrix preparation, data pretreatment, selections of the optimum number of factors and rotational forcing parameter (FPEAK), and the evaluation of PMF solutions was given in Ulbrich et al. (2009) and Zhang et al. (2011a). In this study, the organic mass spectra from *m/z* 12 to *m/z* 125 were used for the PMF analysis. Because of the absence of collocated measurements, the two factor solution with fpeak = 0 and Q/Q_{exp} close to 1 was chosen (see Fig. ~~S1~~ S2 for the PMF diagnostic plots). The two factors including a biomass burning OA (BBOA) and an oxygenated OA (OOA) were identified. The two OA factors showed largely different factor profiles and time series indicating their distinct sources.

3 Results and discussion

3.1 Mass concentration and chemical composition of submicron aerosol

Figure 2 shows a comparison of the total PM_1 mass (NR-PM_1 + BC) with that determined from the SMPS measurements. Assuming spherical particles, the SMPS number concentrations were converted to the mass concentrations using chemically-resolved particle density that was estimated from the chemical composition of PM_1 (Salcedo et al., 2006). As shown in Fig. 2, the time series of PM_1 tracks well with that of SMPS measurements (r^2 = 0.87). The slope of 0.52 is likely due to the limited size range of SMPS measurements (12 – 478 nm) by missing a considerable fraction of large particles that ACSM can measure. The PM_1 mass varied dramatically throughout the study with hourly average concentration ranging from 1.0 to 78.4 μg m^{-3}. The average mass concentration of PM_1 (±1σ) for the entire study is 11.9 (± 8.5) μg m^{-3}, which is ~3 – 4 times lower than those observed at rural sites in China (29.9 – 44.1 μg m^{-3}) (Huang et al., 2011; Hu et al., 2013; Huang et al., 2013; Zhang et al., 2014). It is also approximately twice lower than that (24.5 μg m^{-3}) measured at an urban site in Lanzhou in the Tibetan Plateau (Xu et al., 2014a). While

the average PM_1 mass concentration in this study is close to those observed at the remote sites in Asia, e.g., Okinawa (14.5 μg m^{-3}) (Zhang et al., 2007a) and Fukue (12.0 μg m^{-3}) (Takami et al., 2005) in Japan, and Jeju (8.6 μg m^{-3}) in Korea (Topping et al., 2004), it is much higher than those reported at rural/remote sites in north America and Europe, e.g., Chebogue (2.9 μg m^{-3}), Storm Peak (2.1 μg m^{-3}) and Hyytiala (2.0 μg m^{-3}), and even comparable to the loadings at urban sites, e.g., New York City (12 μg m^{-3}), Pittsburgh (15 μg m^{-3}), Manchester (14.0 μg m^{-3}) (Zhang et al., 2007a). These results suggest that the NBS is a typical rural site in Asia, yet with higher background concentrations compared to those in other continents.

Figure 3 shows the time series of mass concentrations and mass fractions of aerosol species in PM_1. The average PM_1 composition is dominated by organics and sulfate on average accounting for 43% and 28%, respectively. Black carbon and chloride represent small fractions contributing 4.5% and 1.2%, respectively to PM_1. As shown in Fig. 1, the aerosol composition at the NBS is largely different from that observed at the urban site in the Tibetan Plateau (Xu et al., 2014a). In particular, sulfate shows ~60% higher contribution, yet BC is more than twice lower than that observed at the urban site (Fig. 1). Xu et al. (2014a) found that 47% of BC was from local traffic emissions which well explained the higher contribution of BC at the urban site. Compared to this study, the average composition of PM_1 measured by the AMS at other rural sites in China showed similar dominance of sulfate (25 – 34%) except Changdao Island (19%), yet overall higher contributions of nitrate because most these rural sites are close to urban areas with high NO_x emissions. The sulfate contributions become more dominant (36 – 64%) at remote sites in East Asia which are far away from urban areas. The increase of sulfate contribution is associated with a large reduction of nitrate contribution (< 5%). Such a change in aerosol bulk composition at rural/remote sites in East Asia is shown Fig. 1. Overall, organics comprises the major fraction of PM_1, contributing approximately one third of the total mass at most sites. While sulfate plays a dominant role in PM_1 at remote sites, nitrate shows the highest contribution at the rural sites in eastern China. Such compositional differences illustrate the different sources of sulfate and nitrate. While sulfate is

dominantly from regional sources and transport, nitrate is more likely influenced by anthropogenic NO_x emissions over a smaller regional areas.

Aerosol species also varied dramatically throughout the study. For example, the organics increased rapidly from 2.9 μg m^{-3} to 77.8 μg m^{-3} in one hour on 21 September. While sulfate remained small variations, nitrate, chloride, and BC showed similar steep increases as organics indicating strong impacts of local biomass burning (Zhang et al., 2015). Rapid decreases of aerosol species due to the precipitation of scavenging or wind direction change were also frequently observed. For a better understanding aerosol composition under variable meteorological conditions and sources, five episodes with two of them from clean periods are shown in Fig. 3d. The aerosol composition varied largely among different episodes. While the average PM_1 mass concentrations during the two clean episodes are similar (3.6 and 3.8 μg m^{-3}), the episode of Clean2 shows much higher contribution of organics (48% vs. 34%) with slightly lower sulfate (33% vs. 36%) than Clean 1, consistent with their different air mass trajectories (Fig. ~~S2~~S3). The other three episodes show ~5 – 8 times higher mass concentration of PM_1 (17.6 – 27.2 μg m^{-3}) than the two clean episodes. The Ep1 is dominated by organics (70%), almost twice of those during the other two episodes suggesting a largely different source. The relative contributions of sulfate and organics during Ep2 and Ep3 are different although the nitrate contribution is similar. These results suggest that the national background site is subject to the influences of air masses from different sources, some of which are enriched with OA while others are dominated with aerosols mainly composed of ammonium sulfates. We also noticed that the two clean periods showed overall higher contribution of sulfate and lower contribution of nitrate compared to the three pollution episodes. The possible reasons were likely due to that the air masses during clean periods were either from a longer transport when ammonium nitrate was deposited or evaporated due to dilution processes, or from less anthropogenic influenced regions with low NO_x emissions.

The aerosol particle acidity was evaluated using the ratio of measured NH_4^+ ($NH_4^+_{meas}$) to the predicted NH_4^+ ($NH_4^+_{pred}$ = 18×(2×SO_4 /96+NO_3/62+Cl/35.5) that needs to fully neutralize sulfate, nitrate, and chloride (Zhang et al., 2007b). The

$NH_4^+{}_{meas}$ correlates tightly with $NH_4^+{}_{pred}$ (r^2 = 0.95), yielding a regression slope of 0.80. The results suggest that aerosol particles at the NBS are overall acidic. Similar acidic particles were also observed at other rural sites in China, e.g., Jiaxing in Yangtze River Delta (Huang et al., 2013), Kaiping in Pearl River Delta (Huang et al., 2011), ~~and~~ Yufa in Beijing (Takegawa et al., 2009), and Qilianshan Mountain in the northeast of the Qinghai–Xizang Plateau (Xu et al., 2015). As a comparison, the aerosol particles in the urban city Lanzhou in the Tibetan Plateau were overall neutralized (Xu et al., 2014a). ~~The results indicate that aerosol particle acidity has changed during the transport.~~ One of the explanations is that more SO_2 is oxidized to sulfate during the transport while gaseous ammonia is not enough to neutralize the newly formed sulfate. This is supported by the overall higher contribution of sulfate at rural/remote sites than that at urban sites. Also note that the newly formed sulfate particles during the frequent NPF events might also have played a role.

3.2 Diurnal variations

The diurnal cycles of aerosol species and PM_1 are shown in Fig. 4a. The PM_1 shows a pronounced diurnal cycle with the concentration ranging from 7.9 to 13.4 μg m^{-3}. The PM_1 shows a visible peak at noon time and then has a gradual decrease reaching the minimum approximately at 16:00. After that, the PM_1 starts to build up and reaches the highest level at midnight. Such a diurnal cycle is similar to those of SO_2 and CO (Fig. 4d), which likely indicates that the major source of PM_1 at the NBS is from regional transport. All aerosol species present similarly pronounced diurnal cycles to PM_1 with the lowest concentrations occurring approximately at 16:00, indicating that the diurnal cycles of aerosol species were mainly driven by the dynamics of planetary boundary layer. Organics dominated PM_1 composition throughout the day varying from 38% - 51%. The concentration of organics at 16:00 is approximately twice lower than that at midnight. Sulfate shows the largest noon peak among all aerosol species, consistent with those of SO_2 and CO. The sulfate contributes more than 25% to PM_1 with the highest contribution as much as 33% between 12:00 – 14:00. Nitrate and chloride shows relatively stable concentrations before 11:00 and then gradually decreaseds to low ambient levels during daytime.

Such diurnal variations still exist after considering the dilution effects of boundary layer height using the conserved tracer CO as a reference (Fig. 4c). This indicates that gas-particle partitioning affected by temperature and humidity has played an important role in driving the diurnal variations of nitrate and chloride. Consistently, the nitrate contribution to PM_1 during late afternoon is ~7-8% which is much lower than that (> 12%) in the early morning. The diurnal variation of BC is different from that observed at the urban site in the Tibetan Plateau where the pronounced morning peak due traffic influences was observed (Xu et al., 2014a). In fact, BC has a good correlation with secondary nitrate (r^2 = 0.59) indicating that BC is likely dominantly from regional transport. This is also supported by the low ambient levels of NO_x (2.5 – 5.1 μg m^{-3}). The contribution of BC to PM_1 is relatively constant, which is ~ 4 – 5% throughout the day.

3.3 OA composition and sources

PMF analysis of ACSM OA mass spectra identified two factors, i.e., a biomass burning OA (BBOA) and an oxygenated OA (OOA). The mass spectra and time series of the two OA factors are shown in Fig. 5.

3.3.1 BBOA

The mass spectrum of BBOA resembles to that of standard BBOA (r^2 = 0.82) which is characterized by a prominent peak of *m/z* 60 (1.1% of total signal), a tracer *m/z* for biomass burning aerosols (Aiken et al., 2009; Cubison et al., 2011; Hennigan et al., 2011). The fraction of *m/z* 60 in BBOA (1.1%) is also much higher than ~0.3% in the absence of biomass burning impacts (Cubison et al., 2011). BBOA correlates tightly with *m/z* 60 (r^2 = 0.82) and also chloride (r^2 = 0.52). The ratio of BBOA to *m/z* 60 is 55.6, which is higher than that of fresh BBOA (34.5) measured during the second Fire Lab at Missoula Experiment (FLAME II) (Lee et al., 2010). One of the explanations is that BBOA in the ambient is more aged because the *m/z* 60 related levoglucosan can be rapidly oxidized in the atmosphere (Hennigan et al., 2010). Indeed, Zhang et al. (2015) reported a much higher ratio of aged BBOA to *m/z* 60 (74.8) than fresh BBOA (16.8) during two harvest seasons in Nanjing, China. The time series of BBOA shows periodically large ~~plumes~~peaks, particularly on the days

of 21 and 22 September, which were mainly from the burning of a large amount of straws in the south-west region. Relatively high concentration of BBOA was also observed at the end of the campaign due to the burning of cow dung for heating purpose because of the low temperature. The average concentration of BBOA is 0.8 (± 1.5) μg m^{-3} for the entire study on average accounting for 15% of total OA. Although the average BBOA contribution is much lower than those measured in PRD, e.g., Jiaxing (~3.9 μg m^{-3}, 30.1%) (Huang et al., 2013), Kaiping (~1.36 μg m^{-3}, 24.5%) (Huang et al., 2011), and Shenzhen (~5.2 μg m^{-3}, 29.5%) (He et al., 2011), the contribution of BBOA during some strong BB plumes can reach up to 40%, e.g., 21-22 September, indicating a large impact of biomass burning on OA at the national background site. BBOA showed a pronounced diurnal cycle which is similar to that of chloride (Fig. 5c). The BBOA concentration increased rapidly from 18:00 and reached a maximum in 2 hours, likely indicating that the burning of straws and cow dung mainly occurred during this period of time. As a result, the contribution of BBOA to total OA increased from ~10% to more than 20%.

3.3.2 Oxygenated organic aerosols (OOA)

Similar to previously reported OOA (Zhang et al., 2005), the mass spectrum of OOA in this study is characterized by a prominent *m/z* 44 peak (mainly CO_2^+). The mass spectrum of OOA also resembles to that of low-volatility OOA (r^2 = 0.88) (Ng et al., 2011a), yet with higher fraction of *m/z* 44 (f_{44}). Much higher fraction of *m/z* 44 in ACSM OOA spectrum than that from HR-ToF-AMS was reported recently by a comprehensive evaluation of the ACSM (Fröhlich et al., 2015). The results also showed that f_{44} has minor impacts on the mass concentrations of OOA factors, although it varies largely by a factor of 0.6 – 1.3. The average mass concentration of OOA is 4.1 μg m^{-3}, on average accounting for 85% of total OA. The OOA contribution is much higher than those reported at urban sites in summer (~60%) (Huang et al., 2010; Sun et al., 2012; Xu et al., 2014a), and also higher than those (~70%) observed at rural sites in China (Hu et al., 2013; Huang et al., 2013). These results suggest that organic aerosol ~~at the national background site~~ was highly aged and well processed at the NBS. In addition, aqueous-processing of OA at nighttime

associated with high RH might also played a role in forming the highly oxidized OA. The diurnal cycle of OOA was similar to that of PM_1, which showed a small peak before noon time followed by a subsequent decrease until 16:00. The OOA dominated OA throughout the day varying from 80 – 90%, indicating that OA at the NBS ~~and is~~was mainly composed of secondary organic aerosol.~~–~~

Previous studies have shown the ubiquitously tight correlations between sulfate and highly oxidized OA because of their similar secondary nature over regional scales (Zhang et al., 2005; DeCarlo et al., 2010). While the OOA correlates well with secondary sulfate for most of the time in this study, several periods with largely different correlations were also observed (Fig. 6). As shown in Fig. 5b and ~~Fig. 6~~, the ~~different~~weak correlation events mainly occurred during periods with strong biomass burning impacts were observed. However, it cannot be resolved by extending PMF solution to more than 2 factors because of the limitation of PMF technique in source apportionment analysis. Similar different correlations between sulfate and LV-OOA were also observed during two research flights in Mexico City and the Central Mexican Plateau (DeCarlo et al., 2010). Following the approach suggested by DeCarlo et al. (2010), we performed a post-processing technique with external tracers on the further apportionment of OOA. We first assume that OOA and sulfate have similar sources during periods in the absence of biomass burning impacts, which is supported by their tight correlations (r^2 = 0.74). An average OOA/SO_4 ratio of 1.04, i.e., $(OOA/SO_4)_{NBB}$, was obtained by performing a linear regression analysis on OOA versus SO_4. We then assume that SO_4 is completely from non-biomass burning (NBB) sources during BB-impact periods. This assumption is rational~~rationale~~ because previous studies have found that fresh biomass burning emits a very small or negligible fraction of sulfate (Levin et al., 2010). The sulfate-related OOA can be calculated as $OOA\times [OOA/SO_4]_{NBB}$, and the excess OOA that is from different sources is then determined as:

$$OOA_{post\text{-}processed} = OOA - \text{~~OOA~~}SO_4 \times [OOA/SO_4]_{NBB} \quad (1)$$

Because the post-processed OOA shows high concentrations during BB periods, we conclude that it's very likely an aged BBOA that was mixed with OOA. In fact, the

mass spectrum of $OOA_{post\text{-}processed}$ is similar to that of OOA. The fraction of *m/z* 60 (f_{60}) is 0.29%, which is very close to ~0.3% for non-biomass burning organic aerosol (Aiken et al., 2008). Smog chamber experiments have shown that fresh BBOA can be rapidly oxidized within 3 – 4.5 hours (Hennigan et al., 2011). While f_{44} increases significantly, f_{60} quickly decreases to a value close to ~0.3%. Similarly, a recent study in Nanjing resolved an aged BBOA factor with its spectrum resembling to that of OOA yet with much lower f_{60} (Zhang et al., 2015). The average concentration of aged BBOA is ~~3.9~~0.82 (± ~~4.4~~2.65) μg m^{-3}, accounting for 17% of OA for the entire study. The contribution of aged BBOA is close to that of fresh BBOA, which might indicate that half of BBOA has been aged. Still, the sum of fresh and aged BBOA highly correlates with *m/z* 60 (r^2 = 0.81, slope = 136.1). The fresh and aged BBOA together accounted for 33% of the total OA suggesting that BBOA was a large local source of OA during the observational period. With the post-processing technique, the sulfate-related OOA contributed 67% on average of total OA, which is close to those observed at other rural sites in e.g., Kaiping (Huang et al., 2011) and Changdao (Hu et al., 2013).

3.4 Chemistry of particle growth

Figure 7a shows the evolution of size distributions of particle number concentrations for the entire study. New particle formation and growth events (NPE) were observed almost every day (27 days in 34 days). Most NPE started at ~11:00 (The time of sunrise is 2 hours behind of Beijing standard time) and persisted more than half day except some NPE were interrupted by either precipitation events or strong winds. The average particle number size distributions during NPE and non event days (non-NPE) are shown in Fig. 7b. Both NPE and non-NPE show broad size distributions with higher number concentrations occurring during NPE. Three modes with geometric mean diameter (GMD) peaking at 28 nm, 43 nm, and 104 nm, respectively were resolved using a log-normal distribution fitting (Seinfeld and Pandis, 2006). The largest mode (104 nm) dominated the total number of particles accounting for ~70%. In contrast, the average size distribution during non-NPE was characterized by a bi~~o~~-modal distribution with the GMD peaking at 59 nm and 146 nm, respectively.

437 The peak diameters were shifted to the larger sizes compared to those during NPE.
438 Such a size shift from clean days to polluted days was also observed previously in
439 Beijing (Yue et al., 2010). Also, the two modes showed almost equivalent
440 contributions to the total number of particles. The average particle number
441 concentration for the entire study is 2.4×10^3 cm^{-3}, which is nearly an order of
442 magnitude lower than those reported at rural sites in eastern China (Wu et al., 2007),
443 but close to that (2.03×10^3 cm^{-3}) observed at Mount Waliguan which is a remote site
444 located nearby (Kivekas et al., 2009). The particle size was further segregated into
445 small Aitken mode (20 – 40 nm, $N_{20\text{-}40}$), large Aitken mode (40 – 100 nm, $N_{40\text{-}100}$),
446 and Accumulation mode (100 – 470 nm, N_{Accu}) particles. The time series and diurnal
447 cycles of particle numbers for three different sizes are shown in Fig. 7c, d. The $N_{20\text{-}40}$
448 presented sharp peaks almost in everyday corresponding to new particle formation
449 events. The diurnal cycle of $N_{20\text{-}40}$ showed that the number concentration started to
450 increase at approximately 11:00 (150 cm^{-3}) and reached a maximum at 14:00 (770
451 cm^{-3}). In contrast, the $N_{40\text{-}100}$ and N_{Accu} showed largely different diurnal cycles from
452 that of $N_{20\text{-}40}$, indicating their different sources. In fact, the diurnal cycles of $N_{40\text{-}100}$
453 and N_{Accu} are remarkably similar to those of aerosol species, suggesting that the large
454 particles are more likely from regional transport.

455 Figure 8 shows the diurnal evolution of particle number size distributions, aerosol
456 composition, and gaseous species during NPE and non-NPE days. The particle
457 number size distributions during NPE were characterized by distinct bimodal
458 distributions showing a persistent larger mode with the GMD peaking at ~100 nm,
459 and a smaller mode below 50 nm. The particle growth started at approximately 11:00
460 from ~20 nm, and continued to grow slowly until ~45 nm at mid-night. The maximum
461 size particles can grow in this study is generally smaller than those (~60 – 70 nm)
462 observed at urban and rural sites in Beijing (Wang et al., 2013a), which is likely due
463 to the much lower concentrations of aerosol species and precursors. All aerosol
464 species however showed decreases during the particle growth period between 12:00 –
465 17:00, and the gaseous CO and SO_2 showed similar variations as aerosol species. ~~The~~
466 ~~results indicate that planetary boundary layer had played a dominant role in driving~~

~~the diurnal variations of aerosol compared to the particle growth during this period.~~ By excluding the dilution effect of PBL using CO as a tracer, we found that organics was the only species showing a gradual increase during the particle growth period (Fig. 8a) while other species remained minor changes or even slightly decreased. The contribution of organics to PM_1 also showed a corresponding increase from 40% to 47%. These results suggest that organics might have played a dominant role in particle growth at the national background site. Our conclusion is consistent with the recent findings that organics, particularly oxidized organic aerosol species, play a more important role than ammonium sulfate in particle growth (Dusek et al., 2010; Ehn et al., 2014; Setyan et al., 2014). Also note that the contribution of organics to PM_1 during NPE (~40 – 50%) is overall higher than that during non-NPE (~30 – 40%), while the sulfate contribution is correspondingly lower (~20 – 30% vs. 30 – 40%), which further supports the important role of organics during NPE. The particle growth was mixed with anthropogenic sources from 17:00 which are indicated by synchronous enhancements of both aerosol species and gaseous precursors. One of possible reasons is due to the air mass transport from downwind urban areas.

The diurnal evolution of particle size distributions and aerosol composition during non-NPE is largely different from that during NPE. The particle number size distributions and mass concentrations of aerosol species showed a dramatic variation~~change~~ at noon time (12:00), indicating a very different chemical and/or physical process between the first and the second half day. The aerosol particles showed an evident growth from ~50 nm to 60 nm during the first 6 hours, which is likely a continuation of previous NPE. Compared to the early stage of particle growth during NPE, the particle growth during non-NPE is associated with synchronous increases of both organics and sulfate. The results indicate that both organics and sulfate contribute to the particle growth after mixed with anthropogenic sources from ~18:00 in the previous day.

We further calculated the particle growth rates (GR) for NPE events without interruptions due to meteorological changes using Eq. (2).

$$GR = \frac{\Delta D_m}{\Delta t} \quad (2)$$

where D_m is the geometric mean diameter from the log-normal fitting, ΔD_m is the difference of diameter during the growth period and Δt is the duration of growth time. The calculated GR and the corresponding average chemical composition and fraction of OOA during the growth period are shown in Fig. 9a. The GR ranges from 0.8 nm h^{-1} to 3.2 nm h^{-1} with an average of 2.0 nm h^{-1}. The GR in this study is overall consistent with those observed at remote and/or forest sites (Eisele and McMurry, 1997; Weber et al., 1997), yet generally smaller than those measured at urban and polluted rural sites (Yue et al., 2010; Shen et al., 2011; Zhang et al., 2011b) where abundant condensable vapor and high concentrations of particulate matter facilitate the growth of particles (Wang et al., 2013a). By linking GR to aerosol composition, we found that GR at the background site is positively related to the fraction of oxidized OA, which likely indicate the important role of oxidized secondary organic aerosol in particle growth (Ehn et al., 2014). Zhang et al. (2011b) also observed a tight correlation between OOA and GR in urban Beijing supporting the important role of OOA in particle growth. Further investigation is needed for a better understanding of the role of organic aerosol, particularly oxidized OA, in the new particle formation and particle growth at the regional background site.

4 Conclusions

The aerosol particle composition and particle number size distributions were measured at a national background monitoring station in the Tibetan Plateau (3295 m, a.s.l.) from 5 September to 15 October 2013. The average mass concentration of PM_1 is 11.~~49~~ (± 8.5) μg m^{-3} for the entire study, which is ~~ubiquitously~~ lower than those observed at urban and rural sites in eastern China. Organics constituted the major fraction of PM_1, on average accounting for 43% followed by sulfate (28%) and ammonium~~nitrate~~ (11~~0~~%). Several periods with the contribution of organics as much as 70% due to biomass burning impacts were also observed. All aerosol species presented similar diurnal cycles that were mainly driven by the dynamics of planetary boundary layer and regional transport. PMF source apportionment analysis resolved a

secondary OOA and a primary BBOA. OOA dominated OA composition accounting for 85% on average with the rest being BBOA. A post-processing technique based on the correlation of OOA and sulfate separated an aged BBOA which on average accounted for 17% of OA. New particle formation and particle growth events were frequently observed during this study. The particle growth rates varied from 0.8 to 3.2 nm hr^{-1} with an average growth rate of 2.0 nm hr^{-1}. Organics was found to be the only species with gradually increased contribution to PM_1 during NPE. Also, higher contribution of organics during NPE than non-NPE days was observed. These results potentially illustrate the important role of organics in particle growth. Further analysis showed a positive correlation of particle growth rate with the fraction of OOA suggesting that oxidized OA plays a critical role contributing to the particle growth.

Acknowledgements

This work was supported by the National Natural Science Foundation of China (41375133), the National Key Project of Basic Research (2013CB955801), and the Strategic Priority Research Program (B) of the Chinese Academy of Sciences (Grant No. XDB05020500). We thank the National Station for Background Atmospheric Monitoring for providing the meteorological data and gaseous data.

References

Aiken, A. C., DeCarlo, P. F., Kroll, J. H., Worsnop, D. R., Huffman, J. A., Docherty, K. S., Ulbrich, I. M., Mohr, C., Kimmel, J. R., Sueper, D., Sun, Y., Zhang, Q., Trimborn, A., Northway, M., Ziemann, P. J., Canagaratna, M. R., Onasch, T. B., Alfarra, M. R., Prevot, A. S. H., Dommen, J., Duplissy, J., Metzger, A., Baltensperger, U., and Jimenez, J. L.: O/C and OM/OC ratios of primary, secondary, and ambient organic aerosols with High-Resolution Time-of-Flight Aerosol Mass Spectrometry, Environ. Sci. Technol., 42, 4478-4485, 2008.

Aiken, A. C., Salcedo, D., Cubison, M. J., Huffman, J. A., DeCarlo, P. F., Ulbrich, I. M., Docherty, K. S., Sueper, D., Kimmel, J. R., Worsnop, D. R., Trimborn, A., Northway, M., Stone, E. A., Schauer, J. J., Volkamer, R. M., Fortner, E., de Foy, B., Wang, J., Laskin, A., Shutthanandan, V., Zheng, J., Zhang, R., Gaffney, J., Marley, N. A., Paredes-Miranda, G., Arnott, W. P., Molina, L. T., Sosa, G., and Jimenez, J. L.: Mexico City aerosol analysis during MILAGRO using high resolution aerosol mass spectrometry at the urban supersite (T0) - Part 1: Fine particle composition and organic source apportionment, Atmos. Chem. Phys., 9,

6633-6653, 2009.
Cao, J., Lee, S., Chow, J. C., Watson, J. G., Ho, K., Zhang, R., Jin, Z., Shen, Z., Chen, G., and Kang, Y.: Spatial and seasonal distributions of carbonaceous aerosols over China, J. Geophys. Res., 112, 2007.
Cong, Z., Kang, S., Kawamura, K., Liu, B., Wan, X., Wang, Z., Gao, S., and Fu, P.: Carbonaceous aerosols on the south edge of the Tibetan Plateau: concentrations, seasonality and sources, Atmos. Chem. Phys., 15, 1573-1584, 10.5194/acp-15-1573-2015, 2015.
Cubison, M. J., Ortega, A. M., Hayes, P. L., Farmer, D. K., Day, D., Lechner, M. J., Brune, W. H., Apel, E., Diskin, G. S., Fisher, J. A., Fuelberg, H. E., Hecobian, A., Knapp, D. J., Mikoviny, T., Riemer, D., Sachse, G. W., Sessions, W., Weber, R. J., Weinheimer, A. J., Wisthaler, A., and Jimenez, J. L.: Effects of aging on organic aerosol from open biomass burning smoke in aircraft and laboratory studies, Atmos. Chem. Phys., 11, 12049-12064, 10.5194/acp-11-12049-2011, 2011.
DeCarlo, P. F., Ulbrich, I. M., Crounse, J., de Foy, B., Dunlea, E. J., Aiken, A. C., Knapp, D., Weinheimer, A. J., Campos, T., Wennberg, P. O., and Jimenez, J. L.: Investigation of the sources and processing of organic aerosol over the Central Mexican Plateau from aircraft measurements during MILAGRO, Atmos. Chem. Phys., 10, 5257-5280, 10.5194/acp-10-5257-2010, 2010.
Dusek, U., Frank, G. P., Curtius, J., Drewnick, F., Schneider, J., Kürten, A., Rose, D., Andreae, M. O., Borrmann, S., and Pöschl, U.: Enhanced organic mass fraction and decreased hygroscopicity of cloud condensation nuclei (CCN) during new particle formation events, Geophys. Res. Lett., 37, L03804, 10.1029/2009gl040930, 2010.
Ehn, M., Thornton, J. A., Kleist, E., Sipila, M., Junninen, H., Pullinen, I., Springer, M., Rubach, F., Tillmann, R., Lee, B., Lopez-Hilfiker, F., Andres, S., Acir, I.-H., Rissanen, M., Jokinen, T., Schobesberger, S., Kangasluoma, J., Kontkanen, J., Nieminen, T., Kurten, T., Nielsen, L. B., Jorgensen, S., Kjaergaard, H. G., Canagaratna, M., Maso, M. D., Berndt, T., Petaja, T., Wahner, A., Kerminen, V.-M., Kulmala, M., Worsnop, D. R., Wildt, J., and Mentel, T. F.: A large source of low-volatility secondary organic aerosol, Nature, 506, 476-479, 10.1038/nature13032, 2014.
Eisele, F. L., and McMurry, P. H.: Recent progress in understanding particle nucleation and growth, Philosophical Transactions of the Royal Society B: Biological Sciences, 352, 191-201, 10.1098/rstb.1997.0014, 1997.
Fröhlich, R., Crenn, V., Setyan, A., Belis, C. A., Canonaco, F., Favez, O., Riffault, V., Slowik, J. G., Aas, W., Aijälä, M., Alastuey, A., Artiñano, B., Bonnaire, N., Bozzetti, C., Bressi, M., Carbone, C., Coz, E., Croteau, P. L., Cubison, M. J., Esser-Gietl, J. K., Green, D. C., Gros, V., Heikkinen, L., Herrmann, H., Jayne, J. T., Lunder, C. R., Minguillón, M. C., Močnik, G., O'Dowd, C. D., Ovadnevaite, J., Petralia, E., Poulain, L., Priestman, M., Ripoll, A., Sarda-Estève, R., Wiedensohler, A., Baltensperger, U., Sciare, J., and Prévôt, A. S. H.: ACTRIS ACSM intercomparison – Part 2: Intercomparison of ME-2 organic source apportionment results from 15 individual, co-located aerosol mass spectrometers, Atmos. Meas. Tech. Discuss., 8, 1559-1613, 10.5194/amtd-8-1559-2015, 2015.
Gong, Z., Lan, Z., Xue, L., Zeng, L., He, L., and Huang, X.: Characterization of submicron aerosols in the urban outflow of the central Pearl River Delta region of China, Front. Environ. Sci. Eng., 10.1007/s11783-012-0441-8, 2012.

He, L.-Y., Huang, X.-F., Xue, L., Hu, M., Lin, Y., Zheng, J., Zhang, R., and Zhang, Y.-H.: Submicron aerosol analysis and organic source apportionment in an urban atmosphere in Pearl River Delta of China using high-resolution aerosol mass spectrometry, J. Geophys. Res., 116, 10.1029/2010jd014566, 2011.

Hennigan, C. J., Sullivan, A. P., Collett, J. L., and Robinson, A. L.: Levoglucosan stability in biomass burning particles exposed to hydroxyl radicals, Geophys. Res. Lett., 37, L09806, doi:10.1029/2010GL043088, 2010.

Hennigan, C. J., Miracolo, M. A., Engelhart, G. J., May, A. A., Presto, A. A., Lee, T., Sullivan, A. P., McMeeking, G. R., Coe, H., Wold, C. E., Hao, W. M., Gilman, J. B., Kuster, W. C., de Gouw, J., Schichtel, B. A., Collett, J. L., Kreidenweis, S. M., and Robinson, A. L.: Chemical and physical transformations of organic aerosol from the photo-oxidation of open biomass burning emissions in an environmental chamber, Atmos. Chem. Phys., 11, 7669-7686, 10.5194/acp-11-7669-2011, 2011.

Hu, W. W., Hu, M., Yuan, B., Jimenez, J. L., Tang, Q., Peng, J. F., Hu, W., Shao, M., Wang, M., Zeng, L. M., Wu, Y. S., Gong, Z. H., Huang, X. F., and He, L. Y.: Insights on organic aerosol aging and the influence of coal combustion at a regional receptor site of central eastern China, Atmos. Chem. Phys., 13, 10095-10112, 10.5194/acp-13-10095-2013, 2013.

Huang, X.-F., Xue, L., Tian, X.-D., Shao, W.-W., Sun, T.-L., Gong, Z.-H., Ju, W.-W., Jiang, B., Hu, M., and He, L.-Y.: Highly time-resolved carbonaceous aerosol characterization in Yangtze River Delta of China: composition, mixing state and secondary formation, Atmos. Environ., 64, 200 - 207, 10.1016/j.atmosenv.2012.09.059, 2013.

Huang, X. F., He, L. Y., Hu, M., Canagaratna, M. R., Sun, Y., Zhang, Q., Zhu, T., Xue, L., Zeng, L. W., Liu, X. G., Zhang, Y. H., Jayne, J. T., Ng, N. L., and Worsnop, D. R.: Highly time-resolved chemical characterization of atmospheric submicron particles during 2008 Beijing Olympic Games using an Aerodyne High-Resolution Aerosol Mass Spectrometer, Atmos. Chem. Phys., 10, 8933-8945, 10.5194/acp-10-8933-2010, 2010.

Huang, X. F., He, L. Y., Hu, M., Canagaratna, M. R., Kroll, J. H., Ng, N. L., Zhang, Y. H., Lin, Y., Xue, L., Sun, T. L., Liu, X. G., Shao, M., Jayne, J. T., and Worsnop, D. R.: Characterization of submicron aerosols at a rural site in Pearl River Delta of China using an Aerodyne High-Resolution Aerosol Mass Spectrometer, Atmos. Chem. Phys., 11, 1865-1877, 10.5194/acp-11-1865-2011, 2011.

Huang, X. F., He, L. Y., Xue, L., Sun, T. L., Zeng, L. W., Gong, Z. H., Hu, M., and Zhu, T.: Highly time-resolved chemical characterization of atmospheric fine particles during 2010 Shanghai World Expo, Atmos. Chem. Phys., 12, 4897-4907, 10.5194/acp-12-4897-2012, 2012.

Jacobson, M. Z.: Strong radiative heating due to the mixing state of black carbon in atmospheric aerosols, Nature, 409, 695-697, http://www.nature.com/nature/journal/v409/n6821/suppinfo/409695a0_S1.html, 2001.

Kivekas, N., Sun, J., Zhan, M., Kerminen, V. M., HyvÃ¤rinen, A., Komppula, M., Viisanen, Y., Hong, N., Zhang, Y., Kulmala, M., Zhang, X. C., Deli, G., and Lihavainen, H.: Long term particle size distribution measurements at Mount Waliguan, a high-altitude site in inland China, Atmos. Chem. Phys., 9, 5461-5474, 2009.

Lee, T., Sullivan, A. P., Mack, L., Jimenez, J. L., Kreidenweis, S. M., Onasch, T. B., Worsnop, D. R., Malm, W., Wold, C. E., Hao, W. M., and Collett, J. L.: Chemical Smoke Marker

Emissions During Flaming and Smoldering Phases of Laboratory Open Burning of Wildland Fuels, Aerosol Sci. Technol., 44, i-v, 10.1080/02786826.2010.499884, 2010.
Levin, E. J. T., McMeeking, G. R., Carrico, C. M., Mack, L. E., Kreidenweis, S. M., Wold, C. E., Moosmüller, H., Arnott, W. P., Hao, W. M., Collett, J. L., Jr., and Malm, W. C.: Biomass burning smoke aerosol properties measured during Fire Laboratory at Missoula Experiments (FLAME), J. Geophys. Res., 115, D18210, 10.1029/2009jd013601, 2010.
Li, J. J., Wang, G. H., Wang, X. M., Cao, J. J., Sun, T., Cheng, C. L., Meng, J. J., Hu, T. F., and Liu, S. X.: Abundance, composition and source of atmospheric PM 2.5 at a remote site in the Tibetan Plateau, China, Tellus B, 65, 2013.
Matthew, B. M., Middlebrook, A. M., and Onasch, T. B.: Collection efficiencies in an Aerodyne Aerosol Mass Spectrometer as a function of particle phase for laboratory generated aerosols, Aerosol Sci. Technol., 42, 884-898, 10.1080/02786820802356797, 2008.
Middlebrook, A. M., Bahreini, R., Jimenez, J. L., and Canagaratna, M. R.: Evaluation of Composition-Dependent Collection Efficiencies for the Aerodyne Aerosol Mass Spectrometer using Field Data, Aerosol Sci. Technol., 46, 258-271, 10.1080/02786826.2011.620041, 2012.
Ng, N. L., Canagaratna, M. R., Jimenez, J. L., Zhang, Q., Ulbrich, I. M., and Worsnop, D. R.: Real-time methods for estimating organic component mass concentrations from Aerosol Mass Spectrometer data, Environ. Sci. Technol., 45, 910-916, 10.1021/es102951k, 2011a.
Ng, N. L., Herndon, S. C., Trimborn, A., Canagaratna, M. R., Croteau, P. L., Onasch, T. B., Sueper, D., Worsnop, D. R., Zhang, Q., Sun, Y. L., and Jayne, J. T.: An Aerosol Chemical Speciation Monitor (ACSM) for Routine Monitoring of the Composition and Mass Concentrations of Ambient Aerosol, Aerosol Sci. Technol., 45, 780-794, 10.1080/02786826.2011.560211, 2011b.
Paatero, P., and Tapper, U.: POSITIVE MATRIX FACTORIZATION - A NONNEGATIVE FACTOR MODEL WITH OPTIMAL UTILIZATION OF ERROR-ESTIMATES OF DATA VALUES, Environmetrics, 5, 111-126, 10.1002/env.3170050203, 1994.
Salcedo, D., Onasch, T. B., Dzepina, K., Canagaratna, M., Zhang, Q., Huffman, J., DeCarlo, P., Jayne, J., Mortimer, P., and Worsnop, D. R.: Characterization of ambient aerosols in Mexico City during the MCMA-2003 campaign with Aerosol Mass Spectrometry: results from the CENICA Supersite, Atmos. Chem. Phys., 6, 925-946, 2006.
Seinfeld, J. H., and Pandis, S. N.: Atmos. Chem. Phys.: from Air Pollution to Climate Change, Wiley, John & Sons, Incorporated, New York, 1203 pp., 2006.
Setyan, A., Song, C., Merkel, M., Knighton, W. B., Onasch, T. B., Canagaratna, M. R., Worsnop, D. R., Wiedensohler, A., Shilling, J. E., and Zhang, Q.: Chemistry of new particle growth in mixed urban and biogenic emissions – insights from CARES, Atmos. Chem. Phys., 14, 6477-6494, 10.5194/acp-14-6477-2014, 2014.
Shen, X. J., Sun, J. Y., Zhang, Y. M., Wehner, B., Nowak, A., Tuch, T., Zhang, X. C., Wang, T. T., Zhou, H. G., Zhang, X. L., Dong, F., Birmili, W., and Wiedensohler, A.: First long-term study of particle number size distributions and new particle formation events of regional aerosol in the North China Plain, Atmos. Chem. Phys., 11, 1565-1580, 10.5194/acp-11-1565-2011, 2011.
Sun, J., Zhang, Q., Canagaratna, M. R., Zhang, Y., Ng, N. L., Sun, Y., Jayne, J. T., Zhang, X., Zhang, X., and Worsnop, D. R.: Highly time- and size-resolved characterization of

submicron aerosol particles in Beijing using an Aerodyne Aerosol Mass Spectrometer, Atmos. Environ., 44, 131-140, 2010.

Sun, Y. L., Wang, Z., Dong, H., Yang, T., Li, J., Pan, X., Chen, P., and Jayne, J. T.: Characterization of summer organic and inorganic aerosols in Beijing, China with an Aerosol Chemical Speciation Monitor, Atmos. Environ., 51, 250-259, 10.1016/j.atmosenv.2012.01.013, 2012.

Sun, Y. L., Wang, Z. F., Fu, P. Q., Yang, T., Jiang, Q., Dong, H. B., Li, J., and Jia, J. J.: Aerosol composition, sources and processes during wintertime in Beijing, China, Atmos. Chem. Phys., 13, 4577-4592, 10.5194/acp-13-4577-2013, 2013.

Takami, A., Miyoshi, T., Shimono, A., and Hatakeyama, S.: Chemical composition of fine aerosol measured by AMS at Fukue Island, Japan during APEX period, Atmos. Environ., 39, 4913-4924, 2005.

Takegawa, N., Miyakawa, T., Kuwata, M., Kondo, Y., Zhao, Y., Han, S., Kita, K., Miyazaki, Y., Deng, Z., Xiao, R., Hu, M., van Pinxteren, D., Herrmann, H., Hofzumahaus, A., Holland, F., Wahner, A., Blake, D. R., Sugimoto, N., and Zhu, T.: Variability of submicron aerosol observed at a rural site in Beijing in the summer of 2006, J. Geophys. Res., 114, D00G05, 10.1029/2008jd010857, 2009.

Tie, X., and Cao, J.: Aerosol pollution in China: Present and future impact on environment, Particuology, 7, 426-431, http://dx.doi.org/10.1016/j.partic.2009.09.003, 2009.

Topping, D., Coe, H., McFiggans, G., Burgess, R., Allan, J., Alfarra, M. R., Bower, K., Choularton, T. W., Decesari, S., and Facchini, M. C.: Aerosol chemical characteristics from sampling conducted on the Island of Jeju, Korea during ACE Asia, Atmos. Environ., 38, 2111-2123, 10.1016/j.atmosenv.2004.01.022, 2004.

Ulbrich, I. M., Canagaratna, M. R., Zhang, Q., Worsnop, D. R., and Jimenez, J. L.: Interpretation of organic components from Positive Matrix Factorization of aerosol mass spectrometric data, Atmos. Chem. Phys., 9, 2891-2918, 2009.

Wan, X., Kang, S. C., Wang, Y. S., Xin, J. Y., Liu, B., Guo, Y. H., Wen, T. X., Zhang, G. S., and Cong, Z. Y.: Size distribution of carbonaceous aerosols at a high-altitude site on the central Tibetan Plateau (Nam Co Station, 4730 m a.s.l.), Atmospheric Research, 153, 155-164, 10.1016/j.atmosres.2014.08.008, 2015.

Wang, Z. B., Hu, M., Sun, J. Y., Wu, Z. J., Yue, D. L., Shen, X. J., Zhang, Y. M., Pei, X. Y., Cheng, Y. F., and Wiedensohler, A.: Characteristics of regional new particle formation in urban and regional background environments in the North China Plain, Atmos. Chem. Phys., 13, 12495-12506, 10.5194/acp-13-12495-2013, 2013a.

Wang, Z. B., Hu, M., Wu, Z. J., Yue, D. L., He, L. Y., Huang, X. F., Liu, X. G., and Wiedensohler, A.: Long-term measurements of particle number size distributions and the relationships with air mass history and source apportionment in the summer of Beijing, Atmos. Chem. Phys., 13, 10159-10170, 10.5194/acp-13-10159-2013, 2013b.

Weber, R. J., Marti, J. J., McMurry, P. H., Eisele, F. L., Tanner, D. J., and Jefferson, A.: Measurements of new particle formation and ultrafine particle growth rates at a clean continental site, J. Geophys. Res., 102, 4375, 10.1029/96jd03656, 1997.

Wiedensohler, A., Cheng, Y. F., Nowak, A., Wehner, B., Achtert, P., Berghof, M., Birmili, W., Wu, Z. J., Hu, M., Zhu, T., Takegawa, N., Kita, K., Kondo, Y., Lou, S. R., Hofzumahaus, A., Holland, F., Wahner, A., Gunthe, S. S., Rose, D., Su, H., and Poschl, U.: Rapid aerosol

particle growth and increase of cloud condensation nucleus activity by secondary aerosol formation and condensation: A case study for regional air pollution in northeastern China, J. Geophys. Res.-Atmos., 114, D00g08,10.1029/2008jd010884, 2009.
Wu, Z., Hu, M., Liu, S., Wehner, B., Bauer, S., Ma ßling, A., Wiedensohler, A., Petäjä, T., Dal Maso, M., and Kulmala, M.: New particle formation in Beijing, China: Statistical analysis of a 1-year data set, J. Geophys. Res., 112, 10.1029/2006jd007406, 2007.
Xu, J., Zhang, Q., Chen, M., Ge, X., Ren, J., and Qin, D.: Chemical composition, sources, and processes of urban aerosols during summertime in northwest China: insights from high-resolution aerosol mass spectrometry, Atmos. Chem. Phys., 14, 12593-12611, 10.5194/acp-14-12593-2014, 2014a.
Xu, J. Z., Wang, Z. B., Yu, G. M., Qin, X., Ren, J. W., and Qin, D.: Characteristics of water soluble ionic species in fine particles from a high altitude site on the northern boundary of Tibetan Plateau: Mixture of mineral dust and. anthropogenic aerosol, Atmos. Res., 143, 43-56, 10.1016/j.atmosres.2014.01.018, 2014b.
Xu, J. Z., Zhang, Q., Wang, Z. B., Yu, G. M., Ge, X. L., and Qin, X.: Chemical composition and size distribution of summertime PM2.5 at a high altitude remote location in the northeast of the Qinghai–Xizang (Tibet) Plateau: insights into aerosol sources and processing in free troposphere, Atmos. Chem. Phys., 15, 5069-5081, 10.5194/acp-15-5069-2015, 2015.
Yue, D. L., Hu, M., Zhang, R. Y., Wang, Z. B., Zheng, J., Wu, Z. J., Wiedensohler, A., He, L. Y., Huang, X. F., and Zhu, T.: The roles of sulfuric acid in new particle formation and growth in the mega-city of Beijing, Atmos. Chem. Phys., 10, 4953-4960, 10.5194/acp-10-4953-2010, 2010.
Zhang, Q., Worsnop, D. R., Canagaratna, M. R., and Jimenez, J. L.: Hydrocarbon-like and oxygenated organic aerosols in Pittsburgh: Insights into sources and processes of organic aerosols, Atmos. Chem. Phys., 5, 3289-3311, 2005.
Zhang, Q., Jimenez, J. L., Canagaratna, M. R., Allan, J. D., Coe, H., Ulbrich, I., Alfarra, M. R., Takami, A., Middlebrook, A. M., Sun, Y. L., Dzepina, K., Dunlea, E., Docherty, K., DeCarlo, P. F., Salcedo, D., Onasch, T., Jayne, J. T., Miyoshi, T., Shimono, A., Hatakeyama, S., Takegawa, N., Kondo, Y., Schneider, J., Drewnick, F., Borrmann, S., Weimer, S., Demerjian, K., Williams, P., Bower, K., Bahreini, R., Cottrell, L., Griffin, R. J., Rautiainen, J., Sun, J. Y., Zhang, Y. M., and Worsnop, D. R.: Ubiquity and dominance of oxygenated species in organic aerosols in anthropogenically-influenced Northern Hemisphere midlatitudes, Geophys. Res. Lett., 34, L13801,10.1029/2007gl029979, 2007a.
Zhang, Q., Jimenez, J. L., Worsnop, D. R., and Canagaratna, M.: A case study of urban particle acidity and its effect on secondary organic aerosol, Environ. Sci. Technol., 41, 3213-3219, 2007b.
Zhang, Q., Jimenez, J. L., Canagaratna, M. R., Ulbrich, I. M., Ng, N. L., Worsnop, D. R., and Sun, Y.: Understanding atmospheric organic aerosols via factor analysis of aerosol mass spectrometry: a review, Anal. Bioanal. Chem., 401, 3045-3067, 10.1007/s00216-011-5355-y, 2011a.
Zhang, Y. J., Tang, L. L., Wang, Z., Yu, H. X., Sun, Y. L., Liu, D., Qin, W., Canonaco, F., Prévôt, A. S. H., Zhang, H. L., and Zhou, H. C.: Insights into characteristics, sources, and evolution of submicron aerosols during harvest seasons in the Yangtze River delta region, China,

Atmos. Chem. Phys., 15, 1331-1349, 10.5194/acp-15-1331-2015, 2015.
Zhang, Y. M., Zhang, X. Y., Sun, J. Y., Lin, W. L., Gong, S. L., Shen, X. J., and Yang, S.: Characterization of new particle and secondary aerosol formation during summertime in Beijing, China, Tellus B, 63, 382-394, 10.1111/j.1600-0889.2011.00533.x, 2011b.
Zhang, Y. M., Zhang, X. Y., Sun, J. Y., Hu, G. Y., Shen, X. J., Wang, Y. Q., Wang, T. T., Wang, D. Z., and Zhao, Y.: Chemical composition and mass size distribution of PM₁ at an elevated site in central east China, Atmos. Chem. Phys., 14, 12237-12249, 10.5194/acp-14-12237-2014, 2014.
Zhao, Z. Z., Cao, J. J., Shen, Z. X., Xu, B. Q., Zhu, C. S., Chen, L. W. A., Su, X. L., Liu, S. X., Han, Y. M., Wang, G. H., and Ho, K. F.: Aerosol particles at a high-altitude site on the Southeast Tibetan Plateau, China: Implications for pollution transport from South Asia, J. Geophys. Res.-Atmos., 118, 11360-11375, 10.1002/jgrd.50599, 2013.

Tables

Table 1. A summary of average mass concentrations (μg m^{-3}) of PM_1 species during five episodes and the entire study. The 30 min detection limit (DLs) of the ACSM is also shown (Sun et al., 2012).

	Org	SO_4	NO_3	NH_4	Cl	BC	PM_1
Entire Study	4.9	3.2	1.2	1.4	0.14	0.51	11.9
Clean1	1.2	1.3	0.25	0.58	0.02	0.22	3.6
Clean2	1.8	1.3	0.24	0.45	0.03	-	3.8
Ep1	19.1	2.1	2.7	1.4	0.53	1.4	27.2
Ep2	6.3	5.9	2.0	2.6	0.18	0.57	17.6
Ep3	10.8	6.0	2.9	2.6	0.39	1.0	23.7
DLs	0.54	0.07	0.06	0.25	0.03		

Figure Captions:

Figure 1. Map of the sampling site (Menyuan, Qinghai). Also shown is the chemical composition of submicron aerosols measured at selected rural/remote sites in East Asia except Lanzhou, an urban site in northwest China. The detailed information of the sampling sites is presented in Table S1.

Figure 2. Comparison of the mass concentrations of PM_1 (NR-PM_1 +BC) measured by the ACSM and Aethalometer with that by the SMPS (D_m = 12 – 478 nm): (a) time series and (b) scatter plot.

Figure 3. Time series of (a-c) meteorological variables including T (temperature), RH (relative humidity), Precip. (precipitation), WS (wind speed), WD (wind direction), and Vis (visibility), (d) mass concentrations and (e) mass fractions of PM_1 species . The pie charts show the average chemical composition of PM_1 for five episodes.

Figure 4. Average diurnal cycles of (a) mass concentration; (b) mass fraction of PM_1 species; (c) ratios of aerosol species to CO, and (d) gaseous species. The local sunrise and sunset was around 7:00 and 19:00, respectively.

Figure 5. (a) Mass spectra and (b) time series of mass concentrations of BBOA and OOA. The standard average mass spectra of BBOA and OOA in Ng et al. (2011)are also shown for the comparison. The pie chart in (b) shows the average composition of OA for the entire study.

Figure 6. Scatter plot of OOA versus SO_4 during BB and NBB periods. The data points are color coded by BBOA concentrations. The pie chart shows the average composition of OA with post-processed OOA (= OOA – SO_4× $[OOA/SO_4]_{NBB}$).

Figure 7. (a) The evolution of particle number size distributions; (b) average particle number size distributions during NPE and non-NPE; (c,d) time series and diurnal cycles of particle number concentrations for three different sizes. The log-normal distribution fitting of each mode is shown in (b) as dash lines. The sunrise time was around 7:00.

Figure 8. Diurnal evolution of particle size distributions, aerosol composition, gaseous precursors, and the ratios of aerosol species to CO during (a) NPE and (b) non-NPE. The sunrise time was approximately 7:00.

Figure 9. (a) Time series of OOA/PM_1, particle growth rates, and average chemical composition during particle growth periods; (b) correlation of growth rate with OOA/PM_1. The data points are color coded by the PM_1 mass concentration.

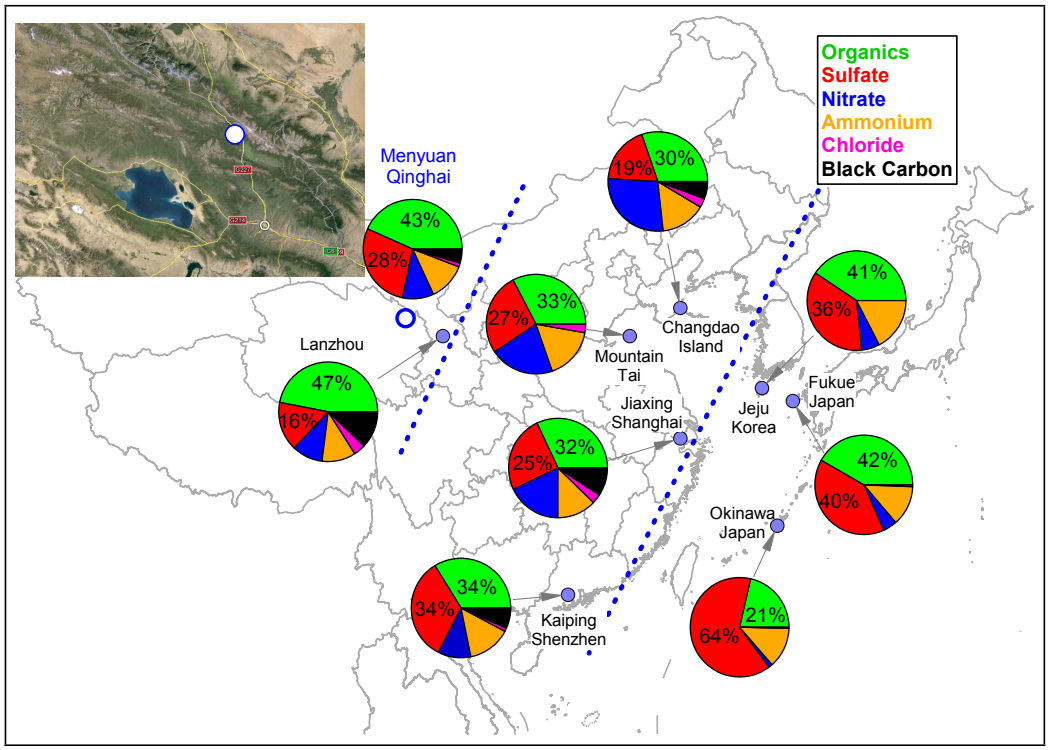

Figure 1. Map of the sampling site (Menyuan, Qinghai). Also shown is the chemical composition of submicron aerosols measured at selected rural/remote sites in East Asia except Lanzhou, an urban site in northwest China. The detailed information of the sampling sites is presented in Table S1.

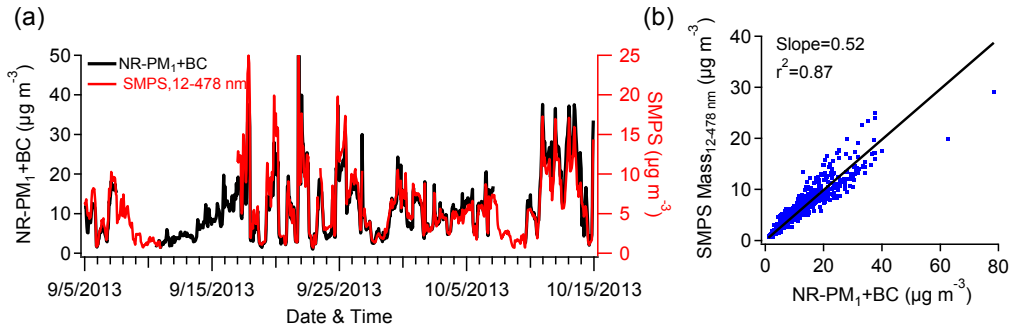

Figure 2. Comparison of the mass concentrations of PM_1 ($NR\text{-}PM_1$ +BC) measured by the ACSM and Aethalometer with that by the SMPS (D_m = 12 – 478 nm): (a) time series and (b) scatter plot.

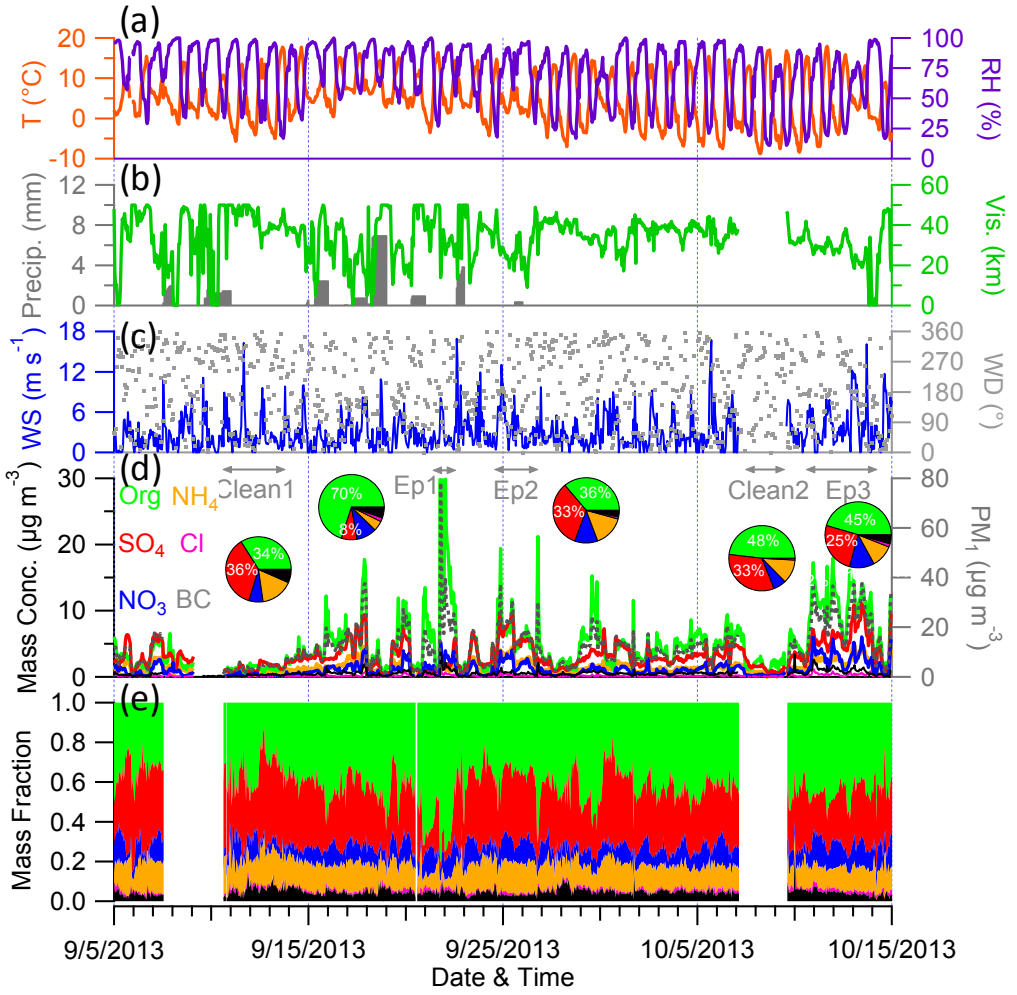

Figure 3. Time series of (a-c) meteorological variables including T (temperature), RH (relative humidity), Precip. (precipitation), WS (wind speed), WD (wind direction), and Vis (visibility), (d) mass concentrations and (e) mass fractions of PM_1 species . The pie charts show the average chemical composition of PM_1 for five episodes.

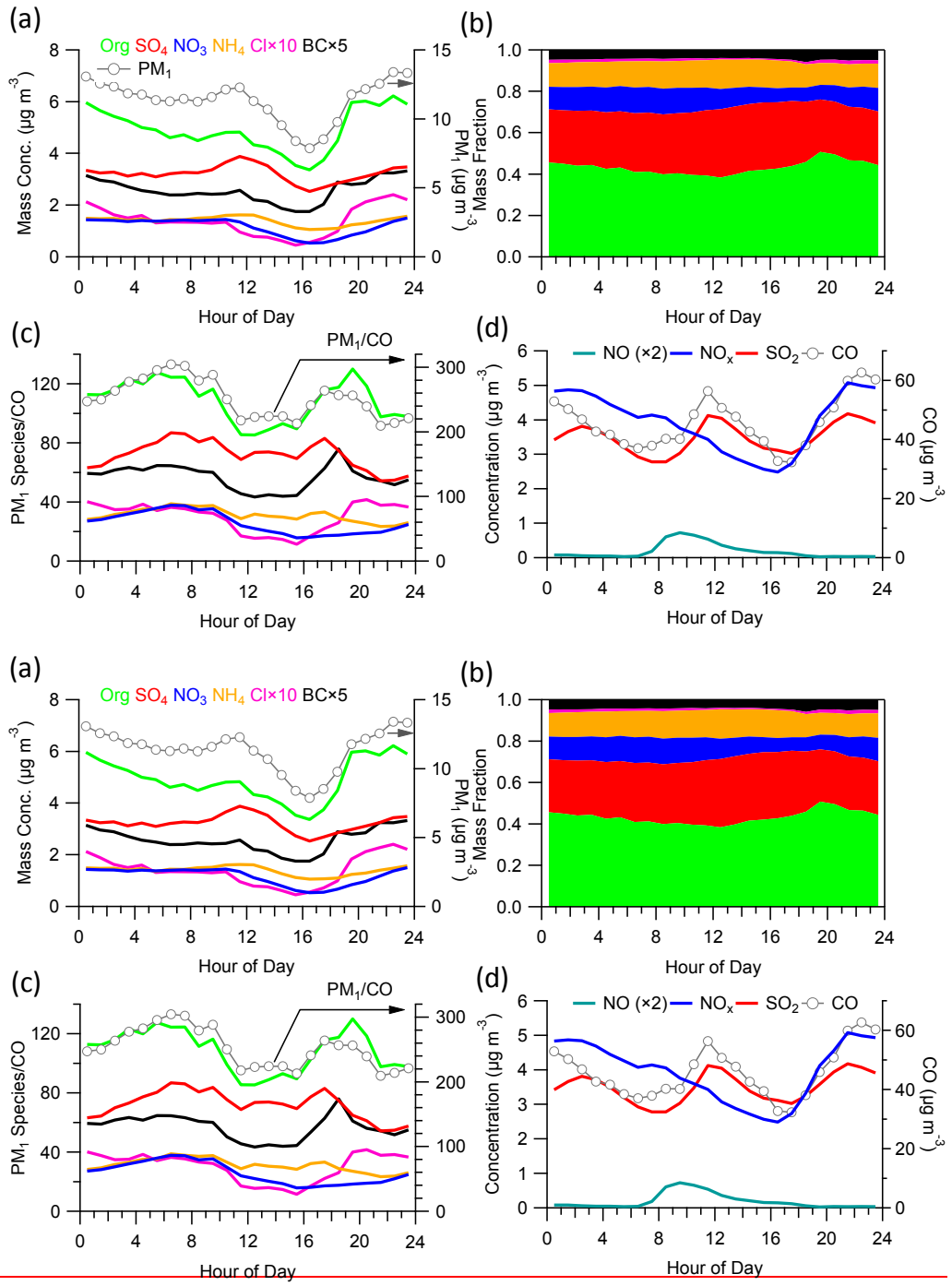

Figure 4. Average diurnal cycles of (a) mass concentration; (b) mass fraction of PM_1 species; (c) ratios of aerosol species to CO, and (d) gaseous species. The local sunrise and sunset was around 7:00 and 19:00, respectively.

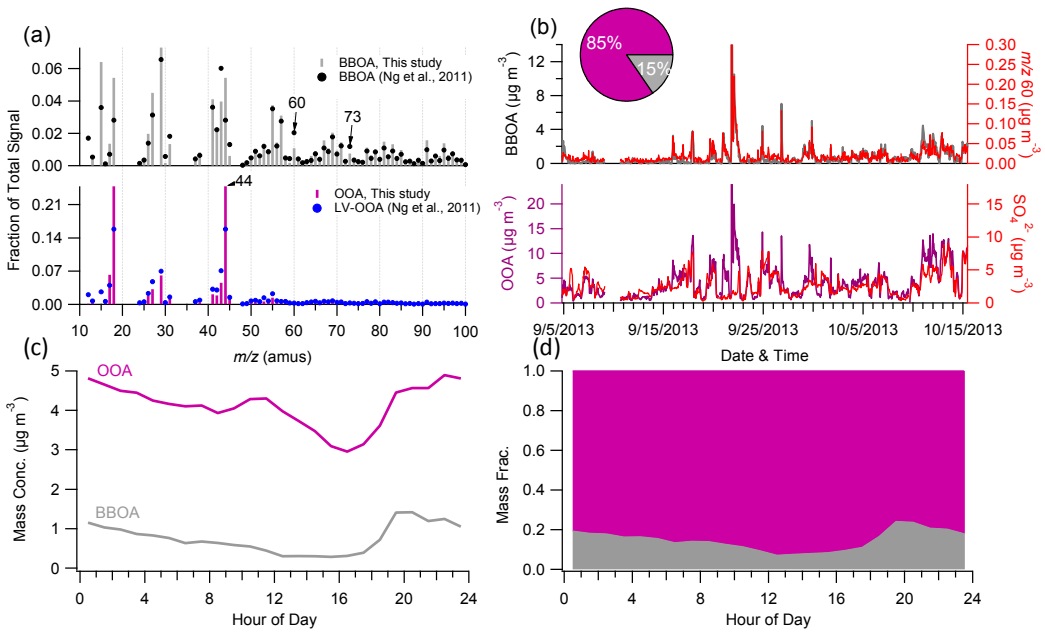

Figure 5. (a) Mass spectra and (b) time series of mass concentrations of BBOA and OOA, (c) and (d) show the average diurnal cycles of BBOA and OOA. In addition, the standard average mass spectra of BBOA and OOA in Ng et al. (2011) are also shown in (a) for the comparison. The pie chart in (b) shows the average composition of OA for the entire study.

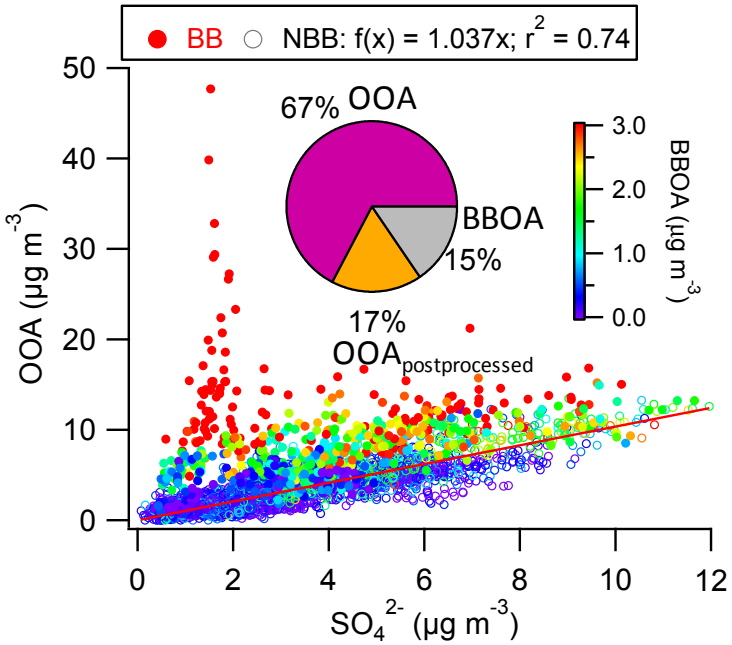

Figure 6. Scatter plot of OOA versus SO_4 during BB and NBB periods. The data points are color coded by BBOA concentrations. The pie chart shows the average composition of OA with post-processed OOA (= OOA – SO_4× $[OOA/SO_4]_{NBB}$).

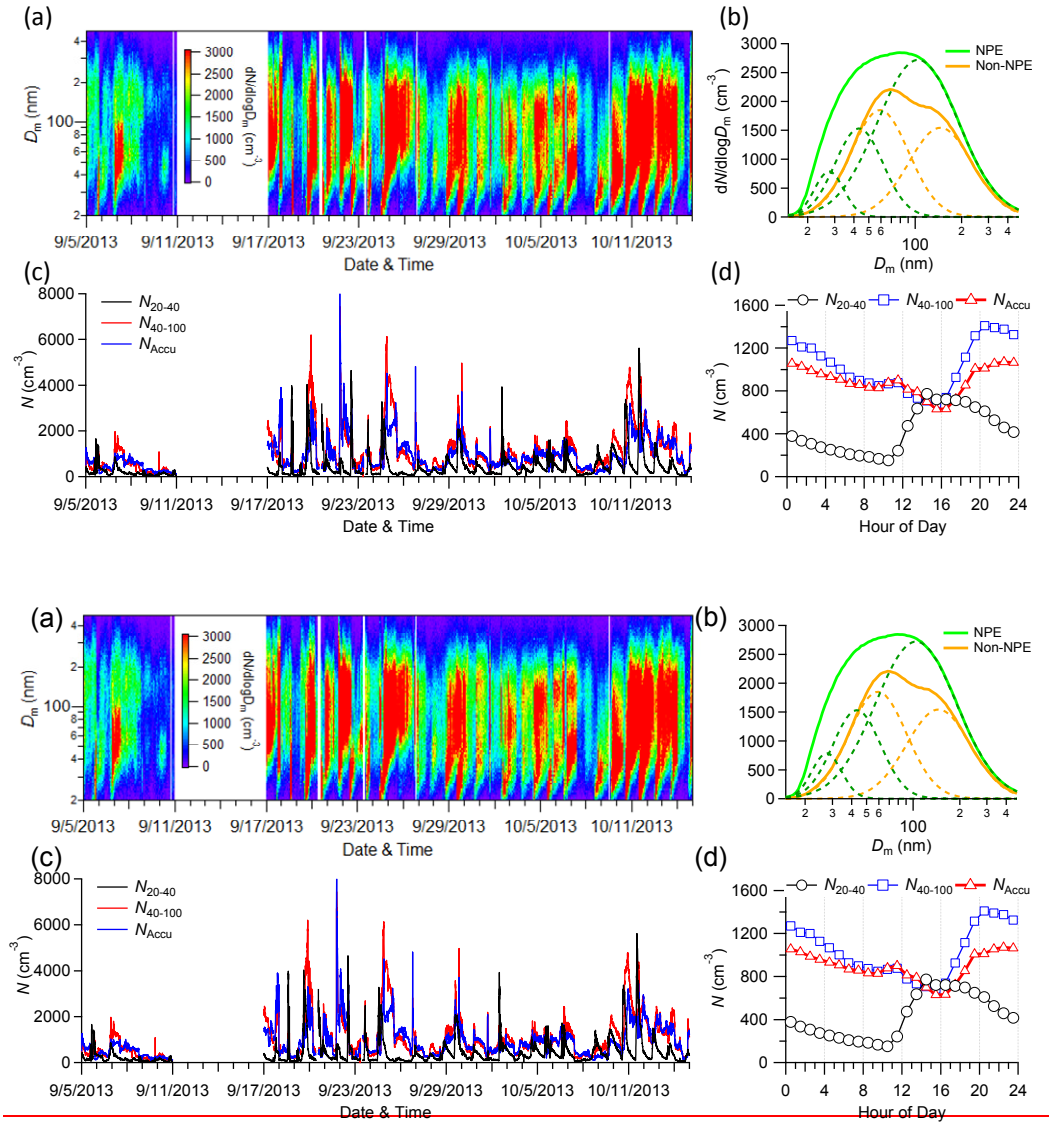

Figure 7. (a) The evolution of particle number size distributions; (b) average particle number size distributions during NPE and non-NPE; (c,d) time series and diurnal cycles of particle number concentrations for three different sizes. The log-normal distribution fitting of each mode is shown in (b) as dash lines. The sunrise time was around 7:00.

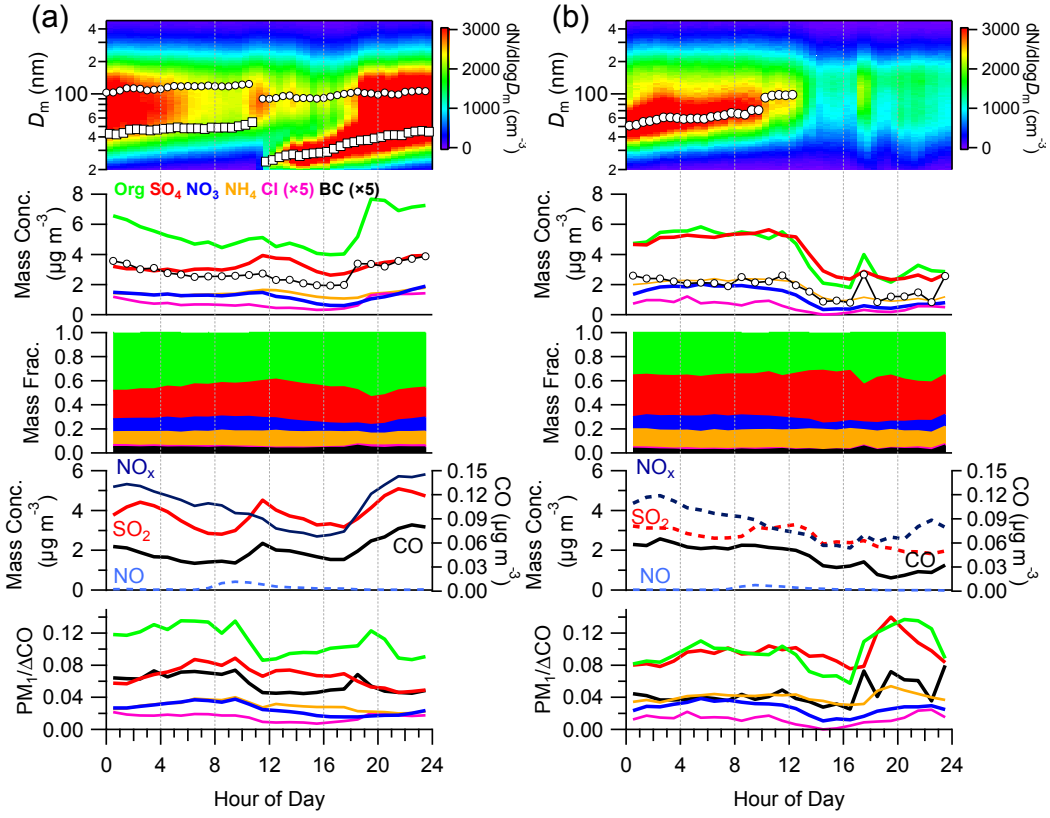
(a)
(b)
D_m (nm)
dN/dlogD_m (cm^{-3})
Org SO_4 NO_3 NH_4 Cl (×5) BC (×5)
Mass Conc. (μg m^{-3})
Mass Frac.
NO_x
SO_2
NO
CO
CO (ng m^{-3})
$PM_1/\Delta CO$
Hour of Day

872

873

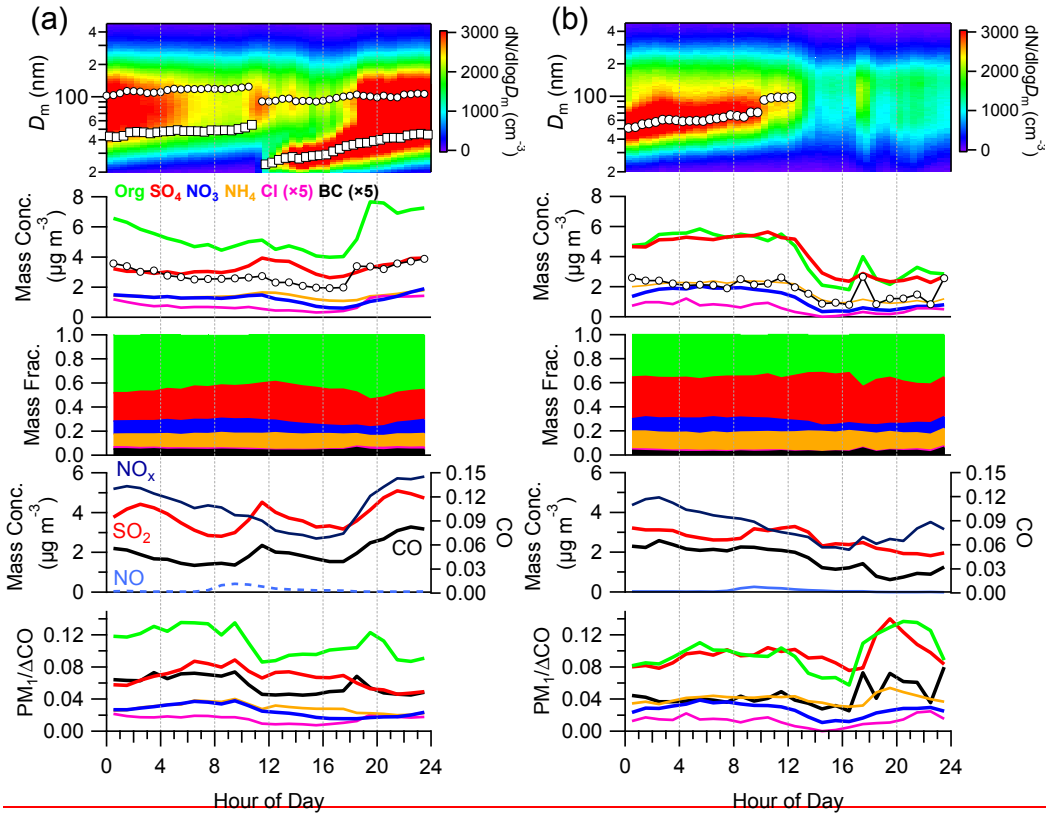
(a)
(b)
D_m (nm)
dN/dlogD_m (cm^{-3})
Org SO_4 NO_3 NH_4 Cl (×5) BC (×5)
Mass Conc. (μg m^{-3})
Mass Frac.
NO_x
SO_2
NO
CO
$PM_1/\Delta CO$
Hour of Day

874

875 Figure 8. Diurnal evolution of particle size distributions, aerosol composition, gaseous
876 precursors, and the ratios of aerosol species to CO during (a) NPE and (b) non-NPE.
877 The sunrise time was approximately 7:00.

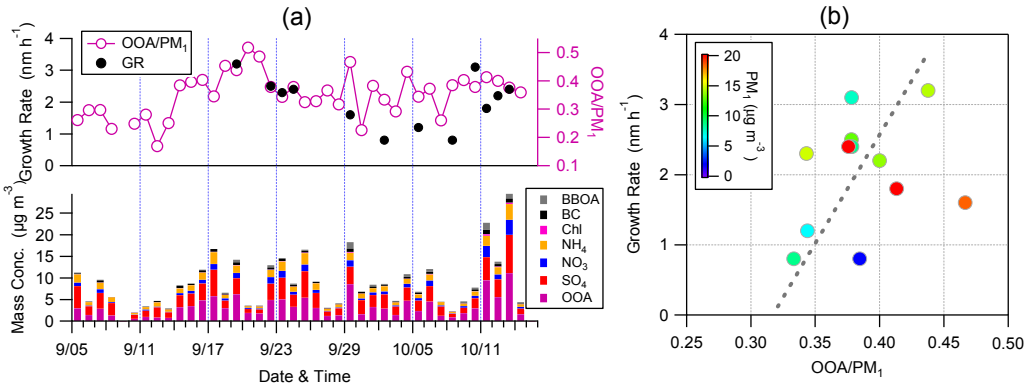

878

879 Figure 9. (a) Time series of OOA/PM_1, particle growth rates, and average chemical
880 composition during particle growth periods; (b) correlation of growth rate with
881 OOA/PM_1. The data points are color coded by the PM_1 mass concentration.